Plant Physiology Preview. Published on December 4, 2017, as DOI:10.1104/pp.17.01369

A single oxidosqualene cyclase produces the seco-triterpenoid α-onocerin

Aldo Almeida[1], Lemeng Dong[1], Bekzod Khakimov[2], Jean-Etienne Bassard[1], Tessa Moses[3,4], Frederic Lota[5], Alain Goossens[3,4], Giovanni Appendino[6] and Søren Bak[1]. (2017)

[1]Department of Plant and Environmental Science, University of Copenhagen, Thorvaldsensvej 40, DK-1871 Frederiksberg C, Denmark.
[2]Department of Food Science, University of Copenhagen, Rolighedsvej 16, DK-1958 Frederiksberg C, Denmark.
[3]Ghent University, Department of Plant Biotechnology and Bioinformatics, Technologiepark 927, 9052 Ghent, Belgium.
[4]VIB Center for Plant Systems Biology, Technologiepark 927, 9052 Ghent, Belgium.
[5]Alkion Biopharma SAS, 4 rue pierre fontaine, 91000, Evry, France.
[6]Dipartimento di Scienze del Farmaco, Università del Piemonte Orientale, Novara, Italy.

Short title not to exceed 50 characters and spaces

Convergent evolution of α-onocerin triterpenoid pathway

Corresponding author(s) details

Søren Bak

bak@plen.ku.dk

Department of Plant and Environmental Science, University of Copenhagen, Thorvaldsensvej 40, DK-1871 Frederiksberg C, Denmark.

One sentence summary

In *Ononis spinosa*, a single oxidosqualene cyclase interacts with squalene epoxidases to produce α-onocerin from squalene-dioxide, demonstrating that α-onocerin pathways evolved convergently in plants.

List of author contributions

Aldo Almeida, Søren Bak and Giovanni Appendino conceived the original research plan.

Aldo Almeida performed most of the experiments, analyzed the data and drafted the paper.

Jean-Etienne Bassard assisted in the design and performance of FLIM experiments.

Bekzod Khakimov provided the GC-MS analysis.

Tessa Moses and Alain Goossens were involved in the yeast expression experiments.

Frederic Lota generated the Hairy-root lines.

Lemeng Dong and Søren Bak supervised and together with Aldo Almeida complemented the writing.

Funding information

The research leading to these results has received funding to TriForC from the European Community's Seventh Framework Programme [FP7/2007-2013] under grant agreement° 613692.

Tessa Moses was supported by the Special Research Funds from Ghent University.

Abstract

8,14-*seco*-triterpenoids are characterized by their unusual open C-ring. Their distribution in nature is rare and scattered in taxonomically unrelated plants. The 8,14-*seco*-triterpenoid α-onocerin is only known from the evolutionarily distant clubmoss genus *Lycopodium* and leguminous genus *Ononis*, which makes the biosynthesis of this *seco*-triterpenoid intriguing from an evolutionary standpoint. In our experiments with *Ononis spinosa,* α-onocerin was detected only in the roots. Through transcriptome analysis of the roots, an oxidosqualene cyclase, OsONS1, was identified that produces α-onocerin from squalene-2,3;22,23-dioxide, when transiently expressed in *Nicotiana bethamiana*. In contrast, in *Lycopodium clavatum* two sequential cyclases LcLCC and LcLCD, are required to produce α-onocerin in the *N. benthamiana* transient expression system. Expression of *OsONS1* in the lanosterol synthase knock-out yeast strain GIL77, which accumulates

squalene-2,3;22,23-dioxide, verified the α-onocerin production. A phylogenetic analysis, predicts that OsONS1 branches off from specific lupeol synthases and does not group with the known *L. clavatum* α-onocerin cyclases. Both the biochemical and phylogenetic analysis of OsONS1 suggest convergent evolution of the α-onocerin pathways. When *OsONS1* was co-expressed in *N. benthamiana* leaves with either of the two *O. spinosa* squalene epoxidases *OsSQE1* or *OsSQE2,* α-onocerin production was boosted, most likely because the epoxidases produce higher amounts of squalene-2,3;22,23-dioxide. Fluorescence Lifetime Imaging Microscopy (FLIM) analysis demonstrated specific protein-protein interactions between OsONS1 with both *O. spinosa* squalene epoxidases. Co-expression of *OsONS1* with the two *OsSQE*s suggests that OsSQE2 is the preferred partner of OsONS1 *in planta*. Our results provide an example of convergent evolution of plant specialized metabolism.

Key words:

α-onocerin, squalene epoxidase, cyclization, convergent evolution, protein-protein interactions

Introduction

Triterpenoids are a class of isoprenoids characterized by an amazing structural diversity. Triterpenoids are mainly derived from the 30-carbon precursor squalene-2,3-oxide (SQO), which is synthesized from squalene by squalene epoxidases (SQEs). The next step in triterpenoid biosynthesis is the cyclization of SQO mediated by oxidosqualene cyclases (OSCs) (Augustin et al., 2011). Cyclization initiates with the acid-catalyzed epoxide ring opening of SQO and continues through a series of methyl and hydride shifts (Abe, 2014) that give a series of conformationally discrete carbocation intermediates (Van Tamelen et al., 1982, Boar et al., 1984). Carbocation shifting in the catalytic cavity of the OSC is a dynamic process (Tian and Eriksson, 2012) that terminates by deprotonation of the carbocation intermediate, resulting in the formation of a neutral compound. Some OSCs deprotonate a single carbocation intermediate, and thus form a single cyclized product, while others have the

plasticity to deprotonate several carbocations at different positions rendering them multi-functional and capable to release multiple cyclized products (Lodeiro et al., 2007, Wu et al., 2008). Thus, OSCs increase triterpenoid diversity by producing distinct triterpenoid skeletons, with over 100 triterpenoid skeletons estimated to originate from their action (Xu et al., 2004).

Seco-triterpenoids are characterized by the presence of an open ring, a structural element that can be directly connected to the cyclization mechanism or result from post-cyclization bond cleavage. In this study, we focused on the *seco*-triterpenoid α-onocerin (Fig. 1), a symmetrical tetracyclic triterpenoid first isolated in 1855 from *Ononis spinosa* (Hlasiwetz, 1855) but only structurally elucidated a century later by Barton and Overton (Barton and Overton, 1955). More than a decade after Barton and Overton's work, α-onocerin was isolated from the club moss *Lycopodium clavatum* (Ageta et al., 1962) as well.

The occurrence of α-onocerin in only two phylogenetically distant branches of the plant kingdom makes the biosynthesis of α-onocerin intriguing from an evolutionary standpoint. In fact, the occurrence of α-onocerin is inconsistent even within the *Ononis* genus. In a survey of α-onocerin accumulation in *Ononis* species, extracts from three species were recorded as lacking α-onocerin, i.e. *O. reclinata*, *O. viscosa* and *O. pusilla* (Rowan and Dean, 1972). Decades later, *O. rotundifolia* was reported as another non α-onocerin producer (Hayes, 2012). The *Ononis* genus is monophyletic and splits into five major clades (Turini et al., 2010); however, there is no clear clustering of *α*-onocerin-producing species as the non-producing species are found in the four major clades that have been tested for α-onocerin accumulation. The simultaneous occurrence of *α*-onocerin-producing and non-producing species in a couple of monophyletic subsections of the genus, such as *O. pubescens* and *O. viscosa* of the *Viscosae* and *O. minutissima* and *O. pusilla* in the *Bugranoides*, suggests that the ancestral species of the *Ononis* genus gained the trait to produce α-onocerin, and that this trait has later been lost in some of the *Ononis* species during the course of evolution. The biological function of *α*-onocerin in *Ononis* species is unknown, however, it is noteworthy that no natural mutant unable to produce *α*-onocerin has been reported for *Ononis spinosa*, implying a strong positive selection for retaining this trait in at least this species.

Assays with *Ononis spinosa* enzyme extracts have shown that α-onocerin is exclusively cyclized from squalene-2,3;22,23-dioxide (SDO) and not the general triterpenoid precursor SQO (Rowan et al., 1971). Accordingly, two key steps for *α*-onocerin biosynthesis are anticipated. First, an efficient squalene epoxidase (SQE) has to provide the cyclase(s) with sufficient amounts of SDO under regular physiological conditions. Squalene epoxidases from different organisms ranging from mammals (Bai et al., 1992) to plants (Rasbery et al., 2007) have been reported to produce SDO, however, only when the subsequent cyclization steps were chemically

inhibited for a couple of hours with AMO-1618 or DMAE-DHA. This inhibition allows the accumulation of SQO and its further conversion to SDO (Field and Holmlund, 1977, Nagumo et al., 1995). The second interesting step in α-onocerin biosynthesis is the cyclization reaction. Recently, it was shown that in *L. clavatum*, biosynthesis of α-onocerin is performed in two steps by two substrate specific OSCs acting sequentially. LcLCC cyclizes SDO to the two ring structure pre-α-onocerin, after which LcLCD initiates cyclization from the remaining epoxide bond of pre-*α*-onocerin to finally produce *α*-onocerin (Araki et al., 2016). However *Lycopodium clavatum* and *Ononis spinosa* are phylogenetically very distant, with the former being a lycopod and the latter an angiosperm. Therefore, it is likely that the α-onocerin pathways have evolved convergently in these two plant species.

Another aspect of triterpenoid biosynthesis that has been overlooked in the literature is the uptake of SQE products by OSCs. It has been suggested that the sterol pathway proceeds by channeling of substrates between each step through micro-domains of the endoplasmic reticulum (ER) (Benveniste, 2004). However, it is known that active SQE and OSC enzymes can localize to related but nevertheless distinct cell compartments, *e.g.* in yeast active SQE is found on/in the ER whereas active lanosterol synthase is found in lipid droplets along with the inactive form of SQE (Athenstaedt et al., 1999, Leber et al., 1998). Aside from probable close proximity of lipid droplets to the ER membrane network, another force driving triterpenoid biosynthesis could be protein-protein interactions. Surprisingly, protein-protein interactions between SQEs and OSCs have not been reported in spite of existing evidence of specific SQE homologs co-expressing with different enzymes of specialized metabolism, specifically OSCs (Suzuki et al., 2002).

In this paper we identify and characterize a single OSC from *O. spinosa* that can produce *α*-onocerin, as well as two SQEs that can boost α-onocerin production upon transient expression in *Nicotiana benthamiana*. In addition, we report protein-protein interactions of the α-onocerin synthase from *O. spinosa* with the SQEs from the same species. Insights into the spatiotemporal contrasts of α-onocerin accumulation and *α*-onocerin biosynthesis in the roots of *O. spinosa* are also provided.

Results

Wild Ononis spinosa accessions accumulate α-onocerin in the roots

To identify plant material suitable for gene discovery in the α-onocerin biosynthetic pathway, accessions of *Ononis spp* were collected from several sources and screened for their α-onocerin content (Table 1). All *O.*

spinosa accessions analyzed contained α-onocerin in the roots but not in aerial tissues, as indicated by Thin-Layer Chromatography (TLC) and Gas Chromatography-Mass Spectrometry (GC-MS) analysis of dichloromethane extracts (Fig. S1A). Extracts from the accession Ont03 (*Ononis natrix*) analyzed by TLC showed a spot on the TLC plate that comigrated with the α-onocerin standard (Fig. S1A), however, GC-MS analysis revealed that it was not α-onocerin (Fig. S1B). The data suggests that *O. natrix* should be added to the list of *Ononis* species that do not produce α-onocerin, as α-onocerin was not detected in any of the three replicates of the three *O. natrix* accessions tested.

The wild accession OsDK7 was selected for pathway elucidation as it displayed high α-onocerin content and seeds were readily available. To determine the optimal OsDK7 root material for gene discovery, accumulation of α-onocerin was monitored across several time points for plants grown hydroponically and in soil (Fig. 1A). In roots of hydroponically grown *O. spinosa* plants the accumulation of α-onocerin was differentially regulated throughout growth. α-Onocerin could not be detected in the roots during early periods of development (15 days after germination), but could be detected in trace amounts 25 days after germination (0.0019±0.0003 $ng \cdot mg^{-1}$ fresh weight). Subsequently a sharp increase was observed 35 days after germination (0.099±0.018 $ng \cdot mg^{-1}$) with the concentration peaking 45 days after germination (0.45±0.04 $ng \cdot mg^{-1}$). α-Onocerin content dropped 60 days after germination to similar levels to those observed at 35 days, and remained in that range 75 days after germination.

α-Onocerin content of OsDK7 plants grown in soil was similarly monitored throughout growth at several time intervals. Sufficient amounts of root tissue could not be obtained from plants 15 and 25 days after germination, and were therefore not analyzed. 35 days after germination, roots contained ~0.18±0.07 $ng \cdot mg^{-1}$ α-onocerin and the accumulation of α-onocerin peaked 45 days after germination (0.56±19 $ng \cdot mg^{-1}$) to levels comparable to those of hydroponically grown plants of the same age.

Finally, *O. spinosa* hairy roots were generated, as it is well know that hairy roots can accumulate elevated levels of plant specialized metabolites, and could thus present an alternative to the hydroponic and soil grown roots. To generate stable hairy root lines, OsDK7 leaf tissue was transformed with *Agrobacterium rhizogenes* strain LBA9402 *virGN54D*. Two hairy root lines, designated Ohry1 and Ohry2 (Fig. S2A and S2B), were obtained that produced α-onocerin. Ohry1 produced ~4 times less α-onocerin than Ohry2 (0.007±0.002 $ng \cdot mg^{-1}$ and 0.029±0.004 $ng \cdot mg^{-1}$ fresh weight, respectively). Nonetheless, α-onocerin production in Ohry2 cultures was still ~15-fold lower than that in 45-day-old hydroponic roots of OsDK7 (Fig. S2C). Consequently, further work was continued with OsDK7 plants grown in the hydroponic system, as they were cleaner and easier to process than those grown in soil and accumulated more α-onocerin than the hairy root lines.

α-*Onocerin accumulates differently in O. spinosa root sections*

To narrow down tissues for transcriptome analysis, we further investigated the accumulation of α-onocerin across the length of *O. spinosa* hydroponically-grown roots at 45 days after germination. The roots where cut in sections and analyzed by TLC (Fig. S1C) and GC-MS (Fig. 1B). A pronounced difference in α-onocerin accumulation was observed across the root length: with the highest content of α-onocerin detected in the root base, the second highest in the mid-section of the root, and only trace amounts were detected in the young roots. α-Onocerin was undetectable in the root tips.

α-*Onocerin is produced by a lupeol synthase-like OSC and its production is boosted by OsSQEs*

For gene discovery, RNA-sequencing was performed on root tips and mid-section roots. Mid-section roots were chosen over basal roots since α-onocerin-pathway genes in mid-section roots were expected to be more actively transcribed than in basal roots, where transcription might have diminished or stopped. A total of 16 million reads were assembled using Trinity, returning a transcriptome of 25,433 predicted genes with an N50 of 1464 bp.

To select SQE candidates, the *O. spinosa* root transcriptome was mined by BLASTN with the two published *Medicago truncatula* SQEs (AJ430609 and AJ430608) as query sequences. Two contigs were retrieved and comparison of the coding sequences showed that they are 94% and 78% identical at the amino acid level to *M. truncatula* monooxygenase 2, respectively. To confirm the sequence of the contigs, RACE was performed on RNA isolated from OsDK7 roots and two distinct full-length transcripts were retrieved that were 82% identical to each other on the amino acid level. *OsSQE1* (GenBank ID: KY625494) showed 91% identity with *M. truncatula* monooxygenase 1, and *OsSQE2* (GenBank ID: KY625495) showed 92% identity to *M. truncatula* monooxygenase 2, at the amino acid level. A maximum-likelihood phylogenetic tree was constructed from the deduced amino acid sequences of theseveral SQEs (Fig. 2A), and showed that the two SQEs from *O. spinosa* clustered with their respective SQE orthologs in *M. truncatula*, indicative of an SQE duplication before the speciation of *M. truncatula* and *O. spinosa*.

To select OSC candidates, the *O. spinosa* root transcriptome was analyzed by BLASTN using a small subset of OSC sequences with defined product profiles as queries. Four contigs were identified: *OsCAS* (GenBank ID: KY657238) showed highest identity to *Pisum sativum* cycloartenol synthase (91% identity at amino acid level),

OsLAS (GenBank ID: KY657237) displayed highest identity to *Arabidopsis thaliana* lanosterol synthase (66%), and *OsBAS* (GenBank ID: KY657236) showed highest identity to *Medicago truncatula* BAS1 β-amyrin synthase (94%). The last contig showed 78% identity to *Glycyrrhiza glabra* lupeol synthase GgLUS1. This contig was considered the most interesting candidate for α-onocerin biosynthesis, since lupeol was not detected in roots or leaves of *O. spinosa*. In addition, lupeol synthases of other species have previously been shown to be multifunctional, i.e. producing diverse products, as is the case for LUP1 and LUP2 from *Arabidopsis thaliana*. RACE was performed on OsDK7 root RNA with gene specific primers designed from the lupeol synthase-like contig, which facilitated isolation and assembly of two distinct transcripts, designated *OsONS1* and *OsONS2*. The principal differences between the transcripts were the length of their 5'UTR sequences (146bp and 29bp, respectively) and 25 SNPs across the whole transcript.

The predicted open reading frames of the four OSC transcripts were transiently expressed in *N. benthamiana* leaves. Five days after infiltration dichloromethane extracts of the infiltrated leaves were analyzed by GC-MS. α-Onocerin was only detected in leaves expressing *OsONS1* or *OsONS2* (Fig. 3A).

When expressed individually in *N. benthamiana* leaves, both *OsONS1* and *OsONS2* transcripts yielded trace amounts of α-onocerin (0.0007±0.0001 and 0.0009±0.0001 ng/mg fresh weight, respectively). As α-onocerin has previously been shown to be produced from SDO and not SQO, we speculated that *N. benthamiana* was not supplying enough SDO to the α-onocerin synthases. Therefore, *OsONS1* and *OsONS2* were co-expressed with either *OsSQE1* or *OsSQE2*. Production of α-onocerin by *OsONS1* and *OsONS2* when co-expressed with *OsSQE2* was increased 7.5- and 4.3-fold, respectively (Fig. 3A). However, OsSQE1 increased the production of α-onocerin of OsONS1 by nearly 20-fold. This α-onocerin boost was also ~2.5 times higher than the α-onocerin-production boost from the combinations: OsONS1+OsSQE2, OsONS2+OsSQE1 and OsONS2+OsSQE2 (Fig. 3A), indicating that the combination of OsSQE1 and OsONS1 is the most performing for α-onocerin biosynthesis.

α-*Onocerin biosynthesis in Ononis spinosa differs from that in Lycopodium clavatum*

To resolve the phylogenic relationship of the *O. spinosa* OSCs, a maximum-likelihood phylogenetic tree was constructed from a multiple sequence alignment of deduced amino acid sequences of a subset of OSCs with confirmed product profiles (Fig. 2B). The phylogenetic tree showed that LcLCC and LcLCD from *L. clavatum*, known to be involved in the production of α-onocerin in this species, stem from sterol metabolism being closely related to *L. clavatum* cycloartenol synthase (LcLCA) (58% and 55% identity at amino acid level, respectively). On the other hand, OsONS1 and OsONS2 from *O. spinosa* branch from angiosperm specialized

246 metabolism from a pre-disposition to lupeol synthesis of the *Fabaceae* family and are distantly related to LcLCC
247 and LcLCD.
248 The *N. benthamiana* transient expression platform was used to compare differences in the α-onocerin
249 biosynthetic pathways of *O. spinosa* and *L. clavatum*. α-Onocerin was not detected when *LcLCC* or *LcLCD* were
250 expressed alone or in combination with *OsSQE1* or *OsSQE2* (Fig. 3B). α-Onocerin accumulation was only
251 detected when *LcLCC* and *LcLCD* were co-expressed together in the presence of either *OsSQE1* or *OsSQE2*. The
252 amount of α-onocerin detected from the *L. clavatum* pathway enzymes was three times less than that of the
253 *OsONS1* and *OsSQE1* combination.
254 To verify the results obtained in *N. benthamiana*, *OsONS1* was expressed in the *erg*7 knock-out yeast strain
255 GIL77. This strain is known to accumulate high amounts of SDO and does not express other OSCs, ensuring that
256 the triterpenoids isolated from the cultures are synthesized solely by the heterologously expressed OSC. GIL77
257 cultures expressing *OsONS1* produced α-onocerin (Fig. 3C), confirming that α-onocerin was biosynthesized by
258 the single cyclase.
259 Biosynthesis of α-onocerin in *L. clavatum* has been shown to require two sequential steps catalyzed by LcLCC
260 and LcLCD. LcLCC first cyclizes SDO to pre-α-onocerin, which is subsequently cyclized by LcLCD to α-onocerin
261 starting the cyclization from the remaining epoxide end (Fig. 4). To evaluate how OsONS1 synthesizes α-
262 onocerin, *in silico* molecular docking simulations were performed. These models aim to establish if OsONS1 can
263 perform the two sequential steps known for *L. clavatum* OSCs, or if it can cyclize both ends of SDO
264 simultaneously in the active site. A homology model of OsONS1 was constructed based on the crystal structure
265 of human lanosterol synthase (HsLAS). The model was evaluated using the Prosaweb server and checked for
266 Ramachandra outliers through the Molprobity server. Correct modeling of the active site was inspected
267 manually. First, the multiple-sequence alignment showed no indication that the active site could protonate
268 both ends of SDO simultaneously since there was no second DCTAE motif (or a similar one). The DCTAE motif is
269 conserved in all OSCs and is responsible for the protonation of the epoxide ring that begins the cyclization
270 cascade. Absence of a second catalytic motif facing the regular DCTAE motif, was confirmed by the homology
271 model (Fig. 4A and B). An alternative for simultaneous cyclization would be if OsONS1 forms a homodimer with
272 the active sites in close proximity facing one another and both ends of SDO are cyclized simultaneously.
273 However, this last hypothesis is unlikely for two reasons. First, the size of SDO in a pre-folded conformation is
274 estimated to be ~6Å, which is too small to span two active sites. Second, the OSCs follow a strict mechanism by
275 which the substrate enters the active site through a substrate channel. Therefore it is more likely that OsONS1
276 is promiscuous for both SDO and pre-α-onocerin. Molecular docking simulations ran for pre-α-onocerin

277 revealed that the molecule could be docked in the active site interacting with the catalytic residue D482 in the
278 OsONS1 protein model at both the cyclized and epoxide ends (Fig. 4A and B). The binding energy for the
279 residue D482 forming a hydrogen bond with the hydroxyl group of pre-α-onocerin was -11.84 kcal·mol^{-1} (Fig.
280 4A) whereas that of D482 interacting with the epoxide end of pre-α-onocerin was -2.32 kcal·mol^{-1} (Fig. 4B). This
281 supported the hypothesis that OsONS1 cyclizes SDO to pre-α-onocerin, which is later diffused out of the active
282 site and then reenters to be cyclized into α-onocerin.
283
284 *OsONS1 and OsSQEs localize to neighboring subcellular compartments and show protein-protein interactions*
285
286 In the *N. benthamiana* co-expression experiments, OsSQE1 boosted α-onocerin production 2.6-fold more than
287 OsSQE2. To determine if α-onocerin production was boosted due to overproduction of SDO by OsSQE1, or if it
288 was due to protein-protein interaction of OsONS1 with the OsSQE1 leading to metabolic channeling, different
289 combinations of N- and C-terminally fluorescently tagged OsONS1 and OsSQEs were co-expressed and analyzed
290 using Fluorescence Lifetime Imaging Microscopy (FLIM).
291 FLIM is a Fluorescence/Förster Resonance Energy Transfer (FRET)-based method to investigate protein-protein
292 interactions, in which measurements are dependent on the fluorophore concentrations. Therefore, for an
293 optimal protein-protein interaction assay, it is generally advised that the least expressed partner is fused to the
294 FRET donor (eGFP tag) and the most expressed partner to the FRET acceptor (mRFP1 tag) (Lalonde et al., 2008).
295 Accordingly, constructs of *OsONS1*, *OsSQE1* and *OsSQE2* fused to *eGFP* at either the N- or C-terminal were
296 prepared. This enabled a qualitative assessment of the expression of the constructs in *N. benthamiana* and
297 additionally revealed the subcellular localization of the enzymes.
298 Confocal images of OsONS1 constructs tagged at both C- and N-terminals showed OsONS1 to be soluble and
299 localized in the cytoplasm, filling the space around the cortical endoplasmic reticulum (ER) (Fig. 5G-I), as well as
300 entering the nucleus (Fig. 5A-C). The addition of the tag at either the N- or C-terminal did not influence the
301 observed localization of OsONS1. In contrast, both OsSQE1 and OsSQE2 tagged at the C-terminal were localized
302 exclusively to the ER network membranes (Fig. 5J-L) and nuclear membrane (Fig. 5D-F). However, when OsSQEs
303 were tagged with eGFP at the N-terminal, no fluorescence was detectable; suggesting that the tag at the N-
304 terminal interfered with expression, stability or localization of the protein. Hence, C-terminally tagged SQEs
305 were used for further FLIM measurements.
306 Overall, confocal imaging revealed that OsSQEs C-terminally tagged with eGFP displayed higher brightness
307 compared to that observed for OsONS1 tagged at either C- or N-terminal, indicating that *OsSQEs* constructs

were expressed higher relative to *OsONS1* constructs. Therefore, constructs of *OsONS1* fused to eGFP at either C- or N-terminal were chosen as the energy donors and *OsSQEs* were fused to mRFP1 at the C-terminal and used as the energy acceptors in subsequent FLIM experiments.

In addition, the functionality of the α-onocerin pathway proteins fused to the fluorescent tags was tested. No α-onocerin was detected when the fusion constructs of OsONS1 were expressed alone in *N. benthamiana* leaves (Fig. 6C and D), suggesting a detrimental effect of the tag on the enzymatic activity of OsONS1. However, when tagged OsONS1 was co-expressed with OsSQE1 or OsSQE2 tagged with mRFP1 at the C-terminal, α-onocerin was detected, with no significant differences in α-onocerin levels between the different combinations. These results indicated that tagged OsONS1 could still produce α-onocerin, but required higher abundance of SDO.

A significant fluorescence lifetime decrease was observed for the donor OsONS1-eGFP in the presence of OsSQE1-mRFP1 as compared to that of OsONS1-eGFP expressed alone, indicating protein-protein interaction between OsONS1 and OsSQE1 (Fig. 6A). A further significant decrease was observed when OsONS1-eGFP was expressed in the presence of OsSQE2-mRFP1. As negative controls OsONS1-eGFP was co-expressed with either the soluble mRFP1 or SbCYP98A1-mRFP1. The latter cytochrome P450 enzyme from *Sorghum bicolor* is unrelated to the triterpenoid pathway but also localizes to the ER membrane. Neither of these controls showed reduction of fluorescence lifetime for OsONS1-eGFP (Fig. 6A), demonstrating that the interactions observed for OsONS1 with OsSQE1 and OsSQE2 are specific.

To investigate whether the tag position influenced the protein-protein interaction, OsONS1 was N-terminally tagged to eGFP and co-expressed in *N. benthamiana* with C-terminally tagged OsSQEs. FLIM results showed that eGFP-OsONS1 fluorescence lifetime was not reduced when co-expressed with the negative controls, but a significant decrease of the fluorescence lifetime values was measured in the presence of OsSQE1-mRFP1, and an even further significant decrease was observed when co-expressed with OsSQE2-mRFP1 (figure 6B).

OsONS1 and OsONS2 co-express with OsSQE2 in O. spinosa root sections

The reduced fluorescence lifetime observed for tagged OsONS1 in the presence of OsSQE2-mRFP1 as compared to that of OsSQE1-mRFP1 in the FLIM experiments is not enough to determine that OsSQE2 had a stronger protein-protein interaction or was the preferred partner of OsONS1. The lower fluorescence lifetime values could be due to the final positioning of fluorescent labels on the proteins with no actual biological significance. In addition, the fact that higher amounts of α-onocerin were detected when OsONS1 was co-

expressed with OsSQE1 in *N. benthamiana* leaves, raises the question whether OsONS1 has a specific partner or if it readily interacts with both OsSQE1 and OsSQE2. Therefore, expression of *OsONSs*, *OsSQE1* and *OsSQE2* was assessed by RT-qPCR in *O. spinosa* root sections and leaf tissues to determine possible co-expression. This analysis showed that the transcript copies of *OsSQE1* were generally three orders of magnitude lower than those of *OsSQE2* in root sections, except in the leaves where *OsSQE1* transcript copies were 2-fold higher than those of *OsSQE2* (Fig. 7). Transcript copies of *OsSQE2* decreased from young root to mid-section roots and further decreased in the basal root. Transcript copies of *OsSQE2* dropped 72-fold in leaf tissue as compared to basal root tissues (Fig. 7B).

A specific primer pair could not be designed to discriminate between *OsONS1* and *OsONS2,* therefore primers were designed in a conserved region to quantify both transcripts simultaneously. The *OsONSs* showed a similar transcript abundance pattern as that of *OsSQE2* across *O. spinosa* root sections. High transcript counts of *OsONSs* were detected in root tips and young roots, subsequently transcript copies of *OsONS*s dropped from young roots by approximately half in mid-section roots and basal roots, finalizing with a ~1400 fold drop from basal root sections to leaf tissue. These data supported that *OsSQE2* may be the specific SQE for α-onocerin biosynthesis and is regulated at a transcriptional level, despite that co-expression in *N. benthamiana* showed that OsSQE1 can boost α-onocerin production of OsONS1 to higher levels than OsSQE2.

Discussion

α-*Onocerin biosynthesis differs in Ononis spinosa and Lycopodium clavatum and is a result of convergent evolution*

Previously it was shown that α-onocerin production in *L. clavatum* proceeds in two cyclization steps (Araki et al., 2016). LcLCC accepts SDO as a substrate and initiates the cyclization cascade from one end of SDO to produce the bicyclic pre-α-onocerin (Fig. 4C), which is in turn cyclized by LcLCD from the remaining epoxide ring to α-onocerin. Here, we show that in *O. spinosa*, a single OSC is capable of producing α-onocerin, in contrast to the previously described two-enzyme system of *L. clavatum*.

The biochemistry and the position of the α-onocerin synthases in the phylogenetic tree strongly indicate that the α-onocerin pathways in these two species evolved convergently. OsONS1 and OsONS2 group with highly specific lupeol synthases of other legumes, such as *Lotus japonicus* and *Glycyrrhiza glabra* (Hayashi et al., 2004,

Sawai et al., 2006). The *Ononis* and *Glycyrrhiza* genera belong to the monophyletic Inverted-repeat-lacking clade (IRLC) in the *Fabaceae* family (Wojciechowski et al., 2004), which is predicted to originate before the *Trifolieae* clade, to which the *Ononis* genus belongs. This suggests that an OSC with pre-disposition for lupeol production could have existed in the common ancestor of the *Ononis* genus and this OSC could have undergone neo-functionalization to be able to produce α-onocerin.

As for the functional mechanism of α-onocerin production by OsONS1, neither multiple sequence alignments of deduced amino acid sequences of OsONSs and characterized OSCs, nor the homology model of OsONS1 show indications of two catalytic motifs (DCTA) facing each other in the active site for simultaneous cyclization of SDO from both ends. This renders it more likely that OsONS1 is a multifunctional enzyme that is able to accept both SDO and pre-α-onocerin and perform the cyclization steps of both LcLCC and LcLCD. Indeed, the multiple sequence alignment of deduced amino acid sequences suggests that synthesis of pre-α-onocerin by OsONS1 is possible, as the residues of OsONSs-L725 correspond to those of yeast lanosterol synthase (Erg7) F699 (Fig. S3). This amino acid is predicted to stabilize the anti-Markovnikov secondary cation for C-ring expansion (Thoma et al., 2004), and changes influencing the position of this amino acid in the catalytic cavity have been reported to give bicyclic products [49]. Since leucine is smaller in size then phenylalanine, this change would enlarge the catalytic cavity and most likely result in destabilization of the anti-Markovnikov secondary cation, thereby disabling C-ring formation. In addition, the literature supports the possibility of OsONS1 being able to perform both cyclization steps. Previous communications reported that lanosterol synthase from rabbit could produce the tetracyclic compound **2** from the semi-cyclic compound **1** (Fig. 4D), thus, providing proof that a "full-pocket fit" is not indispensable for OSC activity, as long as the epoxide required for initiation of the cyclization cascade is present (Van Tamelen et al., 1982). Possibly the substrate specificity of the *L. clavatum* α-onocerin synthases could rely on amino acids in the OSC substrate channel. In fact, α-onocerin synthases of *O. spinosa* differ from those in *L. clavatum* in amino acids that correspond to residues described in the OSC substrate channel, in particular HsLAS C233 and I524 that are both involved in the passage of the substrate to the active site (Thoma et al., 2004), H289 is involved in the hydrogen-bond network of the channel constriction loop (Oliaro-Bosso et al., 2005), and Y237 has been proposed to allow access of the substrate to the catalytic cavity by rotating (Oliaro-Bosso et al., 2011). Lycopods arose early on in the plant phylogeny, hence LcLCC and LcLCD have perhaps had more time for substrate specialization. Conversely, it can be inferred that α-onocerin biosynthesis has appeared more recently in the *Ononis* genus, since OsONSs stem from the highly specific-lupeol-synthase branch of OSCs. The appearance of two distinct α-onocerin synthases could relate to this substrate specialization happening in *O. spinosa*. Future work on site-

400 directed mutagenesis of the above-mentioned residues and *in vitro* studies would provide insights into the
401 specificity of α-onocerin synthases and in OSCs in general.
402
403 *OsSQE1 and OsSQE2 interact specifically with OsONS1 and boost α-onocerin production*
404
405 Previously, Rowan *et al*. (Rowan et al., 1971) established that α-onocerin was produced exclusively from SDO
406 by protein extracts of *O. spinosa* roots. Endogenous SQEs from *N. benthamiana* only provide enough SDO for
407 OsONS1 to produce low amounts of α-onocerin in the transient transformation platform. In this paper we
408 report that two SQEs from *O. spinosa* significantly boost α-onocerin production to different levels in *N.*
409 *benthamiana* and both show protein-protein interactions with OsONS1. The difference in their expression
410 patterns suggests that one of the *OsSQEs* of *O. spinosa* may have specialized for the α-onocerin pathway.
411 Production of SDO appears to be a common feature of SQEs. The lack of substrate specificity of SQEs was
412 previously demonstrated by Van Tamelen and Heys (Van Tamelen and Heys, 1975), while Corey *et al*. (Corey
413 and Russey, 1966) showed that SQE from rat microsomes can epoxidise both ends of squalene. Since then,
414 several SQEs from different mammalian and plant sources have been shown to synthesize SDO *in vitro* (Bai et
415 al., 1992, Rasbery et al., 2007, Nagumo et al., 1995). However, for these epoxidases to generate SDO, SQO
416 must be allowed to accumulate for several hours by inhibiting activity of OSCs (with AMO-1618 or DMAE-DHA)
417 (Nagumo et al., 1995, Field and Holmlund, 1977), suggesting that the rate of SDO production for OsSQEs is
418 different than those reported for the previous SQEs.
419 In addition, the *in planta* role of SDO is not known and it has not been isolated under normal physiological
420 conditions, but only when the catalytic activity of OSCs was inhibited, which leads to an over accumulation of
421 SQO that then can be epoxidized to SDO (Field and Holmlund, 1977, Nagumo et al., 1995). Nonetheless, 24,25-
422 expoxycycloartenol has been reported to occur naturally in tobacco tissue cultures (Schaefer et al., 1970), and
423 this compound is likely to derive from cyclization of SDO by cycloartenol synthase. In human-cell cultures, some
424 oxysterols have been shown to inhibit 3-hydroxy-3-methylglutaryl-coenzyme A reductase (HMGR), suggesting
425 that they have a regulatory role in sterol biosynthesis (Kandutsch et al., 1978, Spencer, 1994). In the *N.*
426 *benthamiana* transient expression experiments, α-onocerin production by OsONS1 was 2.6-fold higher when
427 co-expressed with OsSQE1 than with OsSQE2, in spite of OsSQE2 showing a stronger protein-protein
428 interaction with OsONS1 (Fig. 6A and 6B). These results suggest that the boost in α-onocerin production by
429 *OsONSs* heterologously co-expressed with *OsSQEs* is most likely due to a higher SDO production by the OsSQEs
430 than by the endogenous *N. benthamiana* SQEs. The protein-protein interactions of OsSQEs with OsONS1 would

favor channeling of the SDO to α-onocerin production instead of oxysterols that might halt triterpenoid biosynthesis. In yeast, disruption of the C-4 demethylation complex of Erg25p/Erg26p/Erg27p/Erg28p in *erg*28 mutants reduces ergosterol levels compared to wild-type strains (Gachotte et al., 2001), demonstrating the existence of protein complexes in triterpenoid biosynthesis (Mo et al., 2002), and the importance of protein-protein interactions for metabolic flux in triterpenoid pathways. However, protein-protein interactions among enzymes in the early steps of triterpenoid biosynthesis had not been determined before, in spite of existing indirect evidence such as the C-terminal domain of *Arabidopsis thaliana* squalene synthase being required for efficient channeling of squalene to SQE (Kribii et al., 1997). The results shown here may pave the way for future investigations on the importance of SQEs and their interactions with OSCs in the production of specialized metabolites.

Biosynthesis and accumulation of α*-onocerin differ across root sections*

The FLIM experiments showed OsONS1 to have stronger protein-protein interactions with OsSQE2 than with OsSQE1 (Fig. 6A and 6B). In accordance, *OsONSs* and *OsSQE2* co-expressed across root sections, suggesting that OsSQE2 may be the specific partner of OsONS1 in the α-onocerin pathway. In addition, the FLIM and qRT-PCR data suggests that the root tips and young root sections are the location with highest α-onocerin biosynthetic activity. However, α-onocerin accumulation in the root sections contrasts with the expression patterns observed for the *OsONSs* and *OsSQE2*. While the basal and mid-section roots show highest α-onocerin content they have a lower transcript count for *OsSQE2* and *OsONSs* compared to the root tips and young roots, in which no or only trace amounts of α-onocerin are observed, respectively.

In agreement with *OsSQE2* being the specific partner of *OsONS1*, it was concluded that *MtSQE2* was the specific SQE for saponin metabolism in *M. truncatula*, since it showed co-expression with *β-amyrin synthase* after root cultures were treated with methyl jasmonate (Suzuki et al., 2002). In the same study, *MtSQE1* was found to be lowly expressed in all tissues before or after methyl jasmonate induction. Similarly, in this paper a lower transcript copy number of *OsSQE1* compared to *OsSQE2* is reported in all root sections of *O. spinosa*.

Concerning the distribution of α-onocerin across the roots, analogous specific-spatial accumulation of triterpenoids has been observed in other plants as well. For example, a similar trend was observed for *in vitro* roots of *Peritassa laevigata*, where accumulation of maytenin and 22β-hydroxy-maytenin in the mature root tissue decreased towards the root cap (Pina et al., 2016). However, no gene expression was measured in that study to allow comparing the regulation of biosynthetic genes with that in our study. The discrepancy on the

conjecture of α-onocerin biosynthesis primarily occurring in root tips, but the product accumulating in the basal root can be explained by an active transport of α-onocerin or the absence of special α-onocerin-storing structures in young roots as opposed to mature root sections. The spatial specific distribution of α-onocerin in *O. spinosa* suggests that this compound may have a specific function in the plant, and our results will contribute to the unravelling of the biological function of α-onocerin in *O. spinosa*.

Conclusions

In this paper we characterized two OSCs from *O. spinosa* that are capable of producing α-onocerin when expressed individually in *N. benthamiana* leaves. Expression of *OsONS1* in the yeast strain GIL77 and phylogenetic analysis indicate that the *O. spinosa* α-onocerin synthases arose from a different evolutionary route than those of *L. clavatum*, meaning that the emergence of the α-onocerin pathways in these two species is the result of convergent evolution. In addition, two SQEs of *O. spinosa* specialized for α-onocerin production have been identified and characterized. Both OsSQE1 and OsSQE2 displayed protein-protein interactions with OsONS1 and boosted α-onocerin production of OsONS1 by providing more SDO. The results described in this paper will hopefully foster systematic studies on the convergent evolution of specialized metabolite pathways in unrelated plant species, a puzzling event- especially for compounds like α-onocerin for which a specific biological target or function has not been assigned yet.

Experimental procedures

Plant material

Seeds of wild *O. spinosa* accessions were collected from different locations in the island of Zealand, Denmark or procured from botanical gardens through the Botanic Gardens Conservation International website (https://www.bgci.org/). Commercially available seeds were purchased and details on the origin and labels used throughout this experiment are given in Table 1. The seeds were first nicked using a scalpel, then soaked in water for 48 hours and subsequently transferred to petri dishes that had a wet circular filter paper (Frisenette nr. 118) for them to germinate. After 5 days, seedlings were transferred to either soil (Pindstrup

substrate no. 2) or hydroponic solution (KH_2PO_4 0.2 mM, K_2SO_4 0.2 mM, $MgSO_4.7H_2O$ 0.3mM, NaCl 0.1 mM, $Mg(NO_3)_2.6H_2O$ 0.3 mM, $Ca(NO_3)_2.4H_2O$ 0.9 mM, KNO_3 0.6 mM, and micronutrients Fe(III)-EDTA-Na 0.05mM, $MnCl_2.4H_2O$ 7 µM, $ZnCl_2$ 0.7 µM, $CuSO_4.5H_2O$ 0.8 µM, H_3BO_3 2 µM, $Na_2MoO_4.2H_2O$ 0.8 µM, finally this solution was adjusted to pH 5.5). Plants were grown in the green house with conditions of 16-h day at 18°C and 8-h night at 15°C.

Generation of hairy root lines

Seeds of OsDK7 were washed for 20 min in water with soap, and sterilized in 0.5% bleach for 20 minutes. After rinsing with sterile water for three times, the sterilized seeds were plated on Murashige and Skoog (MS) medium. For hairy-root induction, *Agrobacterium rhizogenes* strains LBA9402, R1200 and Arqua1 were transformed with the modified pJCV51 vector (https://gateway.psb.ugent.be) containing mRFP and a USER™ cloning cassette (NewEngland Biolabs), and selected with spectinomycin resistance. A stripe of a bacterial colony was scraped off with a sterile scalpel blade and resuspended in 20 mL of PS buffer [10 mM PIPES (P8203, Sigma Aldrich)/KOH pH 6.8, 200 mM Sorbitol]. The scalpel was dipped in the suspension and used to make incisions through the leaves, roots, hypocotyl and cotyledons of *in vitro* cultured *O. spinosa*. Incised tissues were placed onto solid MS medium without antibiotics. After growing in the dark for two days, the inoculated tissues were transferred to fresh MS medium supplemented with 500 $\mu g \cdot mL^{-1}$ cefotaxim, 250 $\mu g \cdot mL^{-1}$ carbenicillin, and 50 $\mu g \cdot mL^{-1}$ kanamycin. Then the inoculated leaves were placed back in the dark and were regularly replaced in fresh media containing all antibiotics. After one month, expanding tissues were tested for mRFP fluorescence.

Hairy root lines were imaged using a Leica M205FA fluorescence stereo microscope equipped with a PLAN-APO 1.0x lens (Leica-10450028) and a Leica DFC450C camera. Images were acquired in the LAS 4.0 software (Leica) and scale bars were added using the ImageJ software (Schneider et al., 2012).

Transcriptome analysis and RACE on OSC fragments

The wild accession OsDK7 was grown in hydroponics and at 45 days after germination the roots were cut in sections: root tips (1.5cm from the tip), young root (5cm after root tips), mid-section root (half of the remainder root length) and basal root (remaining root base), tissues were frozen in liquid N_2 and processed immediately. The RNA was isolated from 100mg of root-section tissue using the Spectrum™ Plant total RNA kit

(Sigma-aldrich), and digested with RNase-free DNAse I (Cat. 79254, Qiagen). The root tips of five plants were pooled to have enough tissue for RNA isolation. Quality and quantity of RNA was assayed using the bioanalyzer 2100 (Agilent). Only RNA from root-tips and mid-section roots were shipped to Macrogen sequencing services (Amsterdam, Netherlands) for sequencing with the MiSeq Illumina platform to create pair-end read libraries. Total reads obtained for root tips and mid-section root amounted to 19.68 and 17 million, respectively. Quality of datasets was assayed with FastQC, reads containing and overall quality score below 20 were filtered out using fastx toolkit, and subsequently low-quality bases were trimmed from the ends of the reads using Trimmomatic. For assembling a transcriptome representative of the whole root, the left-end files from root tips and mid-section roots were merged and the same was done for right-end sequence files. The merged files were matched with the paired_sequence_match.py script of paired_sequence_utils 0.1. A total of 16 million reads were input into the Trinity assembler (Grabherr et al., 2011) to obtain the *de novo* assembly of *O. spinosa* root transcriptome. BLAST was downloaded from NCBI and used to blast the transcriptome locally against a small datasets of sequences from previously characterized OSCs and SQEs retrieved from Genbank.

First-strand cDNA was synthesized from total RNA of roots from OsDK7 using the Superscript III first-strand synthesis system (ThermoFisher Scientific). Fragments of OSC were obtained by nested PCR with the degenerate primers 161S, 711A, 463S and 603A (Table S1) following the conditions reported by Kushiro *et al*. (Kushiro et al., 1998). PCR fragments were separated by gel electrophoresis, and the band of ~450 bp was excised and ligated to the pJET1.2 cloning vector (Cat. K1232, ThermoFisher scientific), following the manufacturer's instructions.

We used the SMARTer® cDNA synthesis kit (Clontech, USA) to generate 5'-RACE-ready first strand cDNA and 3' RACE-ready first-strand cDNA, from total RNA of OsDK7 roots, following the manufacturer's instructions. For obtaining the 3' end of OsONS1-2, OsSQE1 and OsSQE2 the 3' template was amplified separately with primers RACE-ONS-F2, RACE-SQE1-F and RACE-SQE2-F, respectively using the Universal primer mix (UPM) as indicated by the manufacturer. For obtaining their 5' end the 5'-template was amplified separately using RACE-ONS-R3, RACE-SQE1-R, RACE-SQE2-R2 (Table S1) and the UPM. PCR conditions for all reactions were an initial denaturation of 95°C for 3 min, then 25 cycles of 95°C for 30 sec, 65°C for 30 sec, 72°C for 3 min, and ended with a final extension of 72°C for 5 min, using the Advantage 2 polymerase mix provided. After gel electrophoresis the bands from each reaction were blunted and ligated to the pJET1.2 cloning vector and transformed into E. coli cells (E. cloni®, Lucigen), several clones of each fragment were cultured and subsequently sequenced. The 3' and 5' sequenced fragments of *OsONS1*, *OsONS2*, *OsSQE1* and *OsSQE2* were aligned using the CLC main work bench v.7 (Qiagen), and were analyzed for the identification of SNPs.

554

555 *Phylogenetic analysis and Homology modeling*

556

557 Sequences of OSCs used for phylogenetic analysis had the following GenBank accession numbers: KY625496
558 (*Ononis spinosa* Onocerin synthase 1, OsONS1), KY625497 (*Ononis spinosa* Onocerin synthase 2, OsONS2),
559 KY657236 (*Ononis spinosa* putative β-amyrin synthase, OsBAS), KY657238 (*Ononis spinosa* putative
560 Cycloartenol synthase, OsCAS), KY657237 (*Ononis spinosa* putative Lanosterol synthase, OsLAS), D89619 (*Pisum*
561 *sativum* cycloartenol synthase, PsCASPEA), AB034802 (*Pisum sativum* β-amyrin synthase, PsOSCPSY), AB034803
562 (*Pisum sativum* mixed-amyrin synthase, PsOSCPSM), AJ430607 (*Medicago truncatula* β-amyrin synthase-,
563 MtBAS1), NM_106546 (*Arabidopsis thaliana* lupeol synthase 1, AtLUP1), NM_106545 (*Arabidopsis thaliana*
564 lupeol synthase 2, AtLUP2), NM_106497 (*Arabidopsis thaliana* seco-oleanane synthase, AtPEN6), NM_123624
565 (*Arabidopsis thaliana* Marneral synthase, AtMRN1), NM_106544 (*Arabidopsis thaliana* β-amyrin synthase,
566 AtBAS), NM_126681 (*Arabidopsis thaliana* cycloartenol synthase, AtCAS1), AB247155 (*Arabidopsis thaliana*
567 Lanosterol synthase, AtLAS1), AB265170 (*Panax ginseng* dammarenediol-II synthase, PgPNA), LC053637
568 (*Lycopodium clavatum* cycloartenol synthase, LcLCA), LC053635 (*Lycopodium clavatum* pre-α-onocerin
569 synthase, LcLCC), LC053636 (*Lycopodium clavatum* onocerin synthase, LcLCD), BAA86930 (*Olea europaea*
570 lupeol synthase, OeOEW), AB116228 (*Glycyrrhiza glabra* lupeol synthase, GgLUS1), AB181245 (*Lotus japonicus*
571 lupeol synthase, LjOSC3), AB244671 (*Lotus japonicus* lanosterol synthase, LjOSC7), AB116238 (*Cucurbita pepo*
572 cucurbitadienol synthase, CpCPQ).
573 Sequences of SQEs used for phylogenetic analysis had the following GenBank accession numbers: KY625494
574 (*Ononis spinosa* squalene epoxidase 1, OsSQE1), KY625495 (*Ononis spinosa* squalene epoxidase 2, OsSQE2),
575 AJ430609 (*Medicago truncatula* mRNA for squalene monooxygenase 1, MtSQE1), AJ430608 (*Medicago*
576 *truncatula* mRNA for squalene monooxygenase 2, MtSQE2), NM_104624 (*Arabidopsis thaliana* squalene
577 epoxidase 1, AtSQE1), NM_127848 (*Arabidopsis thaliana* squalene epoxidase 2, AtSQE2), NM_119938
578 (*Arabidopsis thaliana* squalene epoxidase 3, AtSQE3), XM_001781268 (*Physcomitrella patens* squalene
579 epoxidase, PpSQE).
580 Protein coding sequences were deduced using Expasy translate tool (http://web.expasy.org/translate/). The
581 evolutionary histories for the SQE and OSC protein sequences were inferred separately by using the Maximum-
582 Likelihood method based on the JTT matrix-based model (Jones et al., 1992). The tree with the highest log
583 likelihood was selected (-3976.2379 for the SQE tree and -19047.1377 for the OSC tree). Initial tree(s) for the
584 heuristic search were obtained by applying the Neighbor-Joining method to a matrix of pairwise distances

585 estimated using a JTT model. The trees are drawn to scale, with branch lengths measured in the number of
586 substitutions per site. The analysis involved 8 amino acid sequences and 24 amino acid sequences for the SQE
587 and OSC trees, respectively. All positions containing gaps and missing data were eliminated. In total there were
588 496 and 730 positions in the final datasets for the SQE and OSC trees, respectively. The statistical significance
589 of each node was tested by the bootstrap method using 1,000 iterations. The evolutionary analyses were
590 conducted in MEGA6 (Tamura et al., 2013). Multiple sequence alignments are given in Figure S4.
591 For homology modeling, protein sequences of OsONS1 and Human lanosterol synthase (HsLAS) were aligned
592 using MUSCLE, the alignment was uploaded to the Chimera GUI (Pettersen et al., 2004), and the Modeller
593 (Eswar et al., 2001) integrated tool was used to generate 10 models based on the HsLAS crystal structure (PDB
594 ID code: 1w6k). The models were validated using ProsaWeb (Wiederstein and Sippl, 2007), checked for
595 Ramachandra outliers through the Molprobity server (Davis et al., 2007) and manual inspection in Chimera
596 itself. Chembio3D Ultra 14.0 (Perkin Elmer) was used to create the .mol2 files for pre-α-onocerin to use in
597 Autodock 4 (Morris et al., 2009) for molecular docking simulations.
598 Multiple sequence alignments of OSC proteins for comparison of active residues was done with ClustalW and
599 residues were compared manually from available functional information on OSCs.
600
601 *In planta transient expression in N. benthamiana leaves for triterpenoid analysis*
602
603 The cDNA of *O. spinosa* roots was amplified by PCR using the attB-ONS- primers for *OsONS1* and *OsONS2*, attB-
604 SQE1 primers for *OsSQE1* and attB-SQE2- primers for *OsSQE2* (Table S1). Synthesis of the *LcLCC* and *LcLCD*
605 genes was ordered from GeneArt Gene Synthesis (Invitrogen). The synthetic genes were amplified using attB-
606 LCC and attB-LCD primers (Table S1), and the amplicons Gateway cloned into pDONR 207 (Invitrogen), and
607 subsequently into the pEAQ-HT-DEST expression vector (Sainsbury and Lomonossoff, 2008). All PCR-based
608 constructs were verified by sequencing. Expression constructs were transformed into *Agrobacterium*
609 *tumefaciens* strain AGL1. Colonies of *A. tumefaciens* were picked in the morning and pre-cultured in 5 mL of LB
610 medium with appropriate antibiotics. Afterwards 10 mL of LB containing antibiotics was inoculated with 50 µL
611 of the pre-culture and incubated at 28°C over night or until reaching an OD600 of 1.5. The cultures were
612 centrifuged and the cell pellet resuspended in infiltration buffer (10 mM MgCl2, 10 mM MES, pH 5.6, and 100
613 µM acetosyringone), and OD600 was adjusted to 0.4. The suspension was incubated for 1 h on a shaker at 200
614 rpm at room temperature. Co-infiltration of Agrobacteria was performed with cultures mixed in equal density.
615 *N. benthamiana* plants were grown in soil (Pindstrup substrate no. 2) in a glasshouse with a 16-h day at 28°C

and 8-h night at 28°C photo period. Transient expression assay was performed on 3-week old plants and leaves were harvested 5 days after infiltration, frozen in liquid N_2 and stored at -80°C for further processing.

TLC and GC-MS analysis

α-Onocerin standard was crystallized from air-dried *Ononis spinosa* roots according to (Berger and Sicker, 2009).

All tissues were crushed in N_2 and 100 mg of powder was extracted with 1 ml of dichloromethane for 1h at 37°C shaking (450 rpm). For TLC analysis, 100 µL of this extract was concentrated by aliquoting to a glass vial insert and evaporated under vacuum for 20 min, subsequently redissolving in 20 µL of dichloromethane and loaded on a TLC silica gel 60 F254 (Cat. 105554, Merck). TLC plates were developed with 8:2 chloroform:ethyl acetate solution and α-onocerin was visualized by staining with vanillin-phosphoric acid and heating to 115°C on a heating block.

For GC-MS analysis 50 µL of extract were aliquoted into a glass insert containing 20 µL internal standard (100 µM betulinic acid in methanol) and was evaporated under vacuum. The glass inserts were sealed with air tight magnetic lids into GC–MS vials and derivatized by addition of 30 µl trimethylsilyl cyanide (TMSCN) as described in (Khakimov et al., 2013). All steps involving sample derivatization and injection were automated using a MultiPurpose Sampler (MPS) (Gerstel, Mülheim an der Ruhr, Germany). After reagent addition, the sample was transferred into the agitator of the MPS and incubated at 40 °C for 40 min at 750 rpm. Immediately after derivatization, 1 µl of the derivatized sample was injected in a splitless mode. The spilt/splitless injector port was operated at 320°C. The septum purge flow and purge flow to split vent at 2.1 min after injection were set to 3 and 15 mL/min, respectively. The GC-MS consisted of an Agilent 7890A GC and an Agilent 5975C series MSD (Agilent Technologies, Glostrup, Denmark). GC separation was performed on an Agilent HP-5MS column (30m × 250µm × 0.25µm) by using hydrogen carrier gas at a constant flow rate of 1.2 mL/min. The GC oven temperature program was as follows: initial temperature 40°C, equilibration time 2.0 min, heat up to 270°C at the rate of 12°C/min, then heat at the rate of 6°C/min until 310°C and hold for 10 min. Mass spectra were recorded in the range of 50–700 m/z with a scanning frequency of 2.2 scans sec^{-1}, and the MS detector was switched off during the first 20.0 min of the run since all targeted molecules eluted after this retention time. The transfer line, ion source and quadrupole temperatures were set to 290°C, 230°C and 150°C, respectively. The mass spectrometer was tuned according to manufacturer's recommendation by using perfluorotributylamine (PFTBA). The MPS and GC-MS was controlled using vendor software Maestro (Gerstel).

Expression of OsONS1 in Yeast

LR reaction was performed between pENTR207[OsONS1] vector (previously created for *Nicotiana benthamiana* transient transformation) and pESC-URA-tHMG1-DEST (Fiallos-Jurado et al., 2016) to obtain pESC-URA [GAL10/tHMG1; GAL1/OsONS1] plasmid for expression in yeast. The yeast strain GIL77 (gal2, hem3-6, erg7, ura3-167) was transformed with this plasmid and pre-cultured at 30°C in synthetic defined (SD) medium containing glucose (Clontech) and the uracil drop-out (-U) supplement (Clontech) and supplemented with 20 µg mL^{-1} of ergosterol and 13 µg mL^{-1} of hemin (all from Sigma-Aldrich). After five days, pre-cultures were inoculated in the induction medium SD Gal/Raf-U containing 2% galactose to a starting OD600 of 0.25 and incubated for 72 h. Cells from 1 ml of the culture were collected and lysed using equal volumes of 50% ethanol and 40% KOH according to Moses *et al*. (Moses et al., 2014). The lysate was extracted twice using 500 µL dichloromethane, the organic phases pooled, lyophilized to dryness and derivatized using pyridine and N-methyl-N-(trimethylsilyl)trifluoroacetamide prior to GC-MS analysis.

Absolute quantification by qRT-PCR

Gel electrophoresis confirmed that the primers designed for qRT-PCR (Table S1) amplify only one amplicon. Amplicon sizes for *OsONSs*, *OsSQE1* and *OsSQE2* are 290, 236 and 195 bp, respectively. The amplicons were excised and ligated into pJET1.2 vector. Plasmid concentrations were quantified with a nanodrop (ND-1000). Transcript copy per µL of each fragment inside the pJET1.2 vector was calculated with the equation (Whelan et al., 2003):

$$\text{Number of copies per } \mu\text{L} = \frac{(6.022 \times 10^{23}(\text{copy/mol}) \times \text{DNA amount(g)}}{\text{DNA length (bp)} \times 660\ (\frac{\text{g}}{\text{mol} \cdot \text{bp}})}$$

A 10-fold serial-dilution series ranging from $1x10^6$ to $1x10^{10}$ copies per µl was prepared for each fragment, and to make the standard curves, Ct values were plotted against the log of the copy number.

Each tissue was analyzed in triplicate synthesizing cDNA from 1 µg of total RNA using the Superscript III kit and final volume was adjusted to 10 ng μL^{-1}. All qPCR reactions for the three primer sets were performed in a CFX384™Real-time system (BioRad) under the following conditions: 4 uL PowerUpTM SYBR Green Master Mix (ThermoFisher Scientific), 1 µL of forward primer (2 µM), 1 µL of reverse primer (2 µM), 1 µL of cDNA (10 ng μL^{-}

677 [1]) and 1 µL MilliQ water. The PCR conditions were initial 95°C for 5 min, followed by 40 cycles of 95°C for 15 s,
678 55°C for 15 s and 72°C for 30 s.
679
680 *Protein-protein interaction monitored by Fluorescence Lifetime Imaging Microscopy (FLIM)*
681
682 Preparation of mRFP1 and SbCYP98A1-mRFP1 constructs was described in (Laursen et al., 2016). Construction
683 of *OsONS1*, *OsSQE1* and *OsSQE2* C-terminally fused to eGFP or mRFP1 was done by amplifying the full length
684 coding sequences with appropriate primers (Table S1) and the amplicons was inserted in the
685 pCAMBIA1300/UeGFP vector or pCAMBIA1300/UmRFP1 vector, respectively, by single insert USER™ cloning
686 technique (Geu-Flores et al., 2007). Finally to create the *OsONS1* construct N-terminally fused to eGFP, the full
687 length coding sequence of *OsONS1* was amplified with appropriate primers and the amplicons inserted to the
688 pCAMBIA1300/eGFPU vector (Laursen et al., 2016) with USER™ cloning. For transient expression in *N.*
689 *benthamiana*, constructs were transformed to *Agrobacterium tumefaciens* LBA4404 *virGN54D* (van der Fits et
690 al., 2000). Cultures were prepared as described above but adjusted to final OD_{600} of 0.15. *A. tumefaciens* strains
691 carrying the constructs of interest were co-infiltrated in equal densities with *A. tumefaciens* transformed with a
692 pCAMBIA1300 vector for expression of the viral p19 silencing suppressor protein (2015). Leaf-discs from
693 transformed plants were sampled three days after infiltration for observation by Confocal Laser Scanning
694 Microscopy (CLSM) and FLIM. An SP5x CLSM Microscope equipped with a DM6000 microscope (Leica,
695 Germany) was used for recording images of enzyme subcellular localization with settings described in (Laursen
696 et al., 2016). FLIM was performed by Time-Correlated-Single-Photon Counting (TCSPC) using the Microtime 200
697 system (Picoquant, Germany) and measurements done using an Olympus IX70 microscope (Olympus, Japan),
698 with pulse laser excitation at 485 nm provided by a Picosecond Diode Laser (PDL 828 “SepiaII”, Picoquant) with
699 settings as described in (Laursen et al., 2016). Samples were scanned 232 seconds with the accurate FLIM
700 method on the SymPhoTime64 software (Picoquant). For each combination, measurements were calculated
701 from at least 25 Regions Of Interest (ROIs) from independent images and cells with a threshold of 50 counted
702 photons and a pixel binning of 2. Lifetime value populations were tested for statistical significance by one-way
703 ANOVA/post-hoc Scheffe’s test using IBM SPSS Statistics 24 software.
704
705 **Accession numbers**
706
707 GenBank accession numbers:

KY625496 (*Ononis spinosa* Onocerin synthase 1, OsONS1), KY625497 (*Ononis spinosa* Onocerin synthase 2, OsONS2), KY657236 (*Ononis spinosa* putative β-amyrin synthase, OsBAS), KY657238 (*Ononis spinosa* putative Cycloartenol synthase, OsCAS), KY657237 (*Ononis spinosa* putative Lanosterol synthase, OsLAS), KY625494 (*Ononis spinosa* squalene epoxidase 1, OsSQE1), KY625495 (*Ononis spinosa* squalene epoxidase 2, OsSQE2), D89619 (*Pisum sativum* cycloartenol synthase, PsCASPEA), AB034802 (*Pisum sativum* β-amyrin synthase, PsOSCPSY), AB034803 (*Pisum sativum* mixed-amyrin synthase, PsOSCPSM), AJ430607 (*Medicago truncatula* β-amyrin synthase-, MtBAS1), NM_106546 (*Arabidopsis thaliana* lupeol synthase 1, AtLUP1), NM_106545 (*Arabidopsis thaliana* lupeol synthase 2, AtLUP2), NM_106497 (*Arabidopsis thaliana* seco-oleanane synthase, AtPEN6), NM_123624 (*Arabidopsis thaliana* Marneral synthase, AtMRN1), NM_106544 (*Arabidopsis thaliana* β-amyrin synthase, AtBAS), NM_126681 (*Arabidopsis thaliana* cycloartenol synthase, AtCAS1), AB247155 (*Arabidopsis thaliana* Lanosterol synthase, AtLAS1), AB265170 (*Panax ginseng* dammarenediol-II synthase, PgPNA), LC053637 (*Lycopodium clavatum* cycloartenol synthase, LcLCA), LC053635 (*Lycopodium clavatum* pre-α-onocerin synthase, LcLCC), LC053636 (*Lycopodium clavatum* onocerin synthase, LcLCD), BAA86930 (*Olea europaea* lupeol synthase, OeOEW), AB116228 (*Glycyrrhiza glabra* lupeol synthase, GgLUS1), AB181245 (*Lotus japonicus* lupeol synthase, LjOSC3), AB244671 (*Lotus japonicus* lanosterol synthase, LjOSC7), AB116238 (*Cucurbita pepo* cucurbitadienol synthase, CpCPQ), AJ430609 (*Medicago truncatula* mRNA for squalene monooxygenase 1, MtSQE1), AJ430608 (*Medicago truncatula* mRNA for squalene monooxygenase 2, MtSQE2), NM_104624 (*Arabidopsis thaliana* squalene epoxidase 1, AtSQE1), NM_127848 (*Arabidopsis thaliana* squalene epoxidase 2, AtSQE2), NM_119938 (*Arabidopsis thaliana* squalene epoxidase 3, AtSQE3), XM_001781268 (*Physcomitrella patens* squalene epoxidase, PpSQE).

Supplemental data

Figure S1. α-Onocerin accumulates in the roots of *Ononis spinosa* in a spatial specific manner.

Figure S2. Hairy-root lines induced from *O. spinosa* produce α-onocerin with different levels of accumulation.

Figure S3. Multiple-sequence alignment shows a conserved phenylalanine residue of OSCs is substituted in α-onocerin synthases.

Figure S4. Multiple-sequence alignment of squalene epoxidase and oxidosqualene cyclase deduced protein sequences.

Table S1. Primer list.

Acknowledgements

The research leading to these results has received funding to TriForC from the European Community's Seventh Framework Programme [FP7/2007-2013] under grant agreement° 613692. Tessa Moses was supported by the Special Research Funds from Ghent University.

We thank Dr. Thure Pavlo Hauser for his help in the collection and identification of wild *Ononis spinosa* accessions.

750 **Tables**

751 Table 1. Presence of α-onocerin in the *Ononis spp* accessions sampled

Label	Species	Serial number	α-Onocerin		Source/Location
			Roots	Aerial	
OsDK01	*Ononis spinosa*	Wild	+	-	Mulkholm, Denmark Latitude: 55.674585 Longitude: 11.844718
OsDK02	*Ononis spinosa*	Wild	+	-	Mulkholm, Denmark Latitude: 55.683618 Longitude: 11.829641
OsDK03	*Ononis spinosa*	Wild	+	-	Røsnæs, Denmark Latitude: 55.735394 Longitude: 10.891202
OsDK04	*Ononis spinosa*	Wild	+	-	Røsnæs, Denmark Latitude: 55.733825 Longitude: 10.893441
OsDK05	*Ononis spinosa*	Wild	+	-	Røsnæs, Denmark Latitude: 55.733014 Longitude: 10.894868
OsDK06	*Ononis spinosa*	Wild	+	-	Røsnæs, Denmark Latitude: 55.731662 Longitude: 10.900188
OsDK07	*Ononis spinosa*	Wild	+	-	Nekselø, Denmark Latitude: 55.771877 Longitude: 11.293105
Osp01	*Ononis spinosa*	16847	+	-	Botanische Gärten der Universität Bonn, Germany
Osp02	*Ononis spinosa*	--	+	-	Sheffield seed company, New York, USA
Osp03	*Ononis spinosa*	--	+	-	Jardin des plantes et botanique CAEN, France
Ont01	*Ononis natrix*	199706	-	-	Origin: Madaba, Jordan Maintained by: MSB. Kew royal botanical gardens, UK
Ont02	*Ononis natrix*	122227	-	-	Origin: Zahle, Lebanon Maintained by: MSB. Kew royal botanical gardens, UK
Ont03	*Ononis natrix*	83951	-	-	Origin: Essaouira, Morocco Maintained by: MSB. Kew royal botanical gardens, UK

Figure legends

Figure 1. α-Onocerin content varies throughout plant growth and across the root length. A, Time course of α-onocerin accumulation in root and aerial tissues (fresh weight) of *O. spinosa* plants grown in either soil or hydroponics (Hpn) system. B, Extracted ion chromatograms (480-482m/z) of *O. spinosa* root sections, stem and leaf tissues. C, Mass spectrum of derivatized α-onocerin standard. D, Representative mass spectrum of α-onocerin peak in derivatized extracts from root sections. Values represent means (±standard error) from three biological replicates for each time point, letters indicate significant differences determined by ANOVA/post-hoc Tukey's HSD test at $P<0.05$.

Figure 2. Phylogenetic analysis suggests that the α-onocerin pathway genes in *O. spinosa* and *L. clavatum* are distantly related and arise from convergent evolution. A, Maximum-likelihood tree was constructed on deduced amino acid sequences of eight SQEs aligned by CLUSTALW spanning 496 positions using the MEGA6 program. Statistical significance of each node was tested by the bootstrap method using 1,000 iterations. Representative names: OsSQE1- *Ononis spinosa* squalene epoxidase 1, OsSQE2- *Ononis spinosa* squalene epoxidase 2, MtSQE1- *Medicago truncatula* mRNA for squalene monooxygenase 1, MtSQE2- *Medicago truncatula* mRNA for squalene monooxygenase 2, AtSQE1- *Arabidopsis thaliana* squalene epoxidase 1, AtSQE3- *Arabidopsis thaliana* squalene epoxidase 2, AtSQE3- *Arabidopsis thaliana* squalene epoxidase 3, PpSQE- *Physcomitrella patens* squalene epoxidase.
B, Maximum-likelihood tree was constructed on deduced amino acid sequences 24 OSCs with known product profiles aligned by CLUSTALW spanning 730 positions using the MEGA6 program. Statistical significance of each node was tested by the bootstrap method using 1,000 iterations. Bold letters represent genes from *O. spinosa* and *L. clavatum*. Representative names: OsONS1- *Ononis spinosa* Onocerin synthase 1, OsONS2- *Ononis spinosa* Onocerin synthase 2, OsBAS- *Ononis spinosa* putative β-amyrin synthase, OsCAS- *Ononis spinosa* putative Cycloartenol synthase, OsLAS- *Ononis spinosa* putative Lanosterol synthase, PsCASPEA- (*Pisum sativum* cycloartenol synthase, PsOSCPSY- *Pisum sativum* β-amyrin synthase, PsOSCPSM- *Pisum sativum* mixed-amyrin synthase, MtBAS- *Medicago truncatula* β-amyrin synthase, AtLUP1- *Arabidopsis thaliana* lupeol synthase 1, AtLUP2- *Arabidopsis thaliana* lupeol synthase 2, AtPEN6- *Arabidopsis thaliana seco*- β-amyrin synthase, AtMRN1- *Arabidopsis thaliana* Marneral synthase, AtBAS- *Arabidopsis thaliana* β-amyrin synthase, AtCAS1- *Arabidopsis thaliana* cycloartenol synthase, AtLAS1- *Arabidopsis thaliana* Lanosterol synthase, PgPNA- *Panax ginseng* dammarenediol-II synthase, LcLCA- *Lycopodium clavatum* cycloartenol synthase, LcLCC-

Lycopodium clavatum pre-α-onocerin synthase, LcLCD- *Lycopodium clavatum* onocerin synthase, OeOEW- *Olea europaea* lupeol synthase, GgLUS1- *Glycyrrhiza glabra* lupeol synthase, LjOSC3- *Lotus japonicus* lupeol synthase, LjOSC7- *Lotus japonicus* lanosterol synthase, CpCPQ- *Cucurbita pepo* cucurbitadienol synthase. GenBank ID numbers for each nucleotide sequence of OSCs and SQEs are given in the experimental procedures section.

Figure 3. α-Onocerin biosynthesis in *O. spinosa* is biochemically different from that of *L. clavatum*. A, α-Onocerin content of *N. benthamiana* leaves transiently transformed with *OSCs* and *SQEs* of *O. spinosa*. B, α-Onocerin content of *N. benthamiana* leaves transiently transformed with α-onocerin synthases of *L. clavatum* co-expressed with *SQEs* of *O. spinosa*. C, Total ion chromatogram showing production of α-onocerin in yeast strain GIL77 transformed with *OsONS1* of *O. spinosa*. Values represent means (±standard error) from three biological replicates, letters indicate significant differences determined by ANOVA/post-hoc Tukey's HSD test at $P<0.05$.

Figure 4. Docking simulations of OsONS1 homology model shows pre-α-onocerin can dock from both ends to the catalytic aspartate residue, D482. Color coding: Pink-Carbon atoms of pre-α-onocerin, green: Carbon atoms in amino acid residues of OsONS1 homology model, red: oxygen atoms, blue- nitrogen atoms, white- hydrogen atoms, yellow- sulfur atoms. A, Epoxide end of pre-α-onocerin forming hydrogen bond with catalytic aspartate D482 in active site of OsONS1-homology model. B, Hydroxyl group from cyclized end of pre-α-onocerin forming hydrogen bond with catalytic aspartate D482 in active site of OsONS1-homology model. C, Steps of α-onocerin biosynthetic pathway. D, Demonstrated cyclization reaction by rabbit microsomes. Compound **1:** 3-((3*E*,7*E*)-3,7-dimethyl-10-((8a*S*)-2,5,5,8a-tetramethyl-3,4,4a,5,6,7,8,8a-octahydronaphthalen-1-yl)deca-3,7-dien-1-yl)-2,2-dimethyloxirane and compound **2**: 8,14-*seco*-gammacera-7,14-diene-3-ol.

Figure 5. OsONS1 is localizes in the cytoplasm, while OsSQEs are restricted to the ER membrane as visualized by confocal microscopy of *N. benthamiana* epidermal leaves. Confocal Laser Scanning Microscopy (CLSM) images were collected 3 days after agroinfiltration of *N. benthamiana* leaves. Representative confocal images of the nucleus (A-F) and parietal cell space (G-L) of leaves expressing eGFP-tagged target proteins are shown. Soluble enzymes may permeate through the nuclear pores and be found inside the nucleus (A-C) and fill out the cytoplasm around cortical ER (G-I). ER proteins are restrained to nuclear membranes (D-F) and to a characteristic ER membrane network (J-L). Due to turgescent vacuole pushing the cytoplasm and ER near the

814 plasma membrane, well defined ER network and diffused cytoplasmic patterns may be visualized when
815 observing the cortical space in epidermal cells of *N. benthamiana* leaves. Scale bars = 10 μm.
816
817 Figure 6. OsONS1 interacts with both OsSQE1 and OsSQE2. A, FLIM values for *OsONS1* tagged with *eGFP* on the
818 C-terminal co-expressed with several *mRFP1* fused constructs in transiently transformed *N. benthamiana*
819 leaves. B, FLIM values for *OsONS1* tagged with *eGFP* on the N-terminal co-expressed with several *mRFP1*
820 tagged constructs in transiently transformed *N. benthamiana* leaves. C, α-Onocerin content of *N. benthamiana*
821 leaves transiently transformed with *OsONS1-eGFP* co-expressed with several *mRFP1* tagged constructs. D, α-
822 Onocerin content of *N. benthamiana* leaves transiently transformed with *eGFP-OsONS1* co-expressed with
823 several *mRFP1* tagged constructs. For figures A and B, letters indicate significant differences determined by
824 ANOVA/post-hoc Scheffe's method at $P<0.05$. For figure C and D, Values represent means (±standard error)
825 from three biological replicates, letters indicate significant differences determined by ANOVA/post-hoc Tukey's
826 HSD test at $P<0.05$.
827
828 Figure 7. *OsSQE2* and *OsONSs* co-express across root sections and leaves of *O. spinosa*. A, absolute
829 quantification of *OsSQE1* number of transcripts in different tissues of *O. spinosa*. B, absolute quantification of
830 *OsSQE2* number of transcripts in different tissues of *O. spinosa*. C, absolute quantification of *OsONSs* number
831 of transcripts in different tissues of *O. spinosa*. Reverse Transcription-quantitative PCR was performed on RNA
832 extracted from the pooled tissues of 5 plants. Values represent mean (±standard error) from three different
833 pooling per tissue, letters indicate significant differences determined by ANOVA/post-hoc Tukey's HSD test at
834 $P<0.05$.
835
836 Figure S1. α-Onocerin accumulates in the roots of *Ononis spinosa* in a spatial specific manner. A, Screening of
837 root and leaf tissues from the collected *Ononis* species for presence of α-onocerin by TLC, all accessions of
838 *Ononis spinosa* contain α-onocerin in the roots and not in aerial tissues, accession Ont03 gives a spot that co-
839 migrates with α-onocerin standard. B, Extracted ion chromatogram (480-482m/z) of root and leaf tissues from
840 *Ononis natrix* (Ont03) confirms absence of α-onocerin in this accession. C, Qualitative measurement of α-
841 onocerin accumulation gradient in root sections by TLC.
842
843 Figure S2. Hairy-root lines induced from *O. spinosa* produce α-onocerin with different levels of accumulation. A,
844 Stereomicroscope image of hairy-root line 1 (Ohry1) phenotype. B, Stereomicroscope image of hairy-root line 2

(Ohry2) phenotype. C, α-Onocerin content of hairy-root lines. Values represent means (±standard error) from three biological replicates, asterisk indicates significant difference determined by Student's t-test ($P < 0.05$).

Figure S3. Multiple-sequence alignment shows a conserved phenylalanine residue of OSCs is substituted in α-onocerin synthases. A phenylalanine residue conserved in representative OSCs of other triterpenoid pathways is substituted in α-onocerin synthases from *O. spinosa* and *L. clavatum*. Multiple-sequence alignment of eleven OSCs showing the residue F699 of ScErg7 known to alter cyclization stereochemistry.

Figure S4. Multiple-sequence alignments of squalene epoxidase and oxidosqualene cyclase deduced protein sequences. A, Multiple-sequence alignment of squalene epoxidase deduced protein sequences. B, Multiple-sequence alignment of oxidosqualene cyclases deduced protein sequences.

858 **References**

859

860 2015. Correction. *The Plant Journal,* 83**,** 752-752.
861 ABE, I. 2014. The Oxidosqualene Cyclases: One Substrate, Diverse Products. *Natural Products.* John Wiley &
862 Sons, Inc.
863 AGETA, H., IWATA, K. & OOTAKE, Y. 1962. Isolation of α-onocerin from *Lycopodium clavatum* INN.
864 *CHEMICAL & PHARMACEUTICAL BULLETIN,* 10**,** 637-637.
865 ARAKI, T., SAGA, Y., MARUGAMI, M., OTAKA, J., ARAYA, H., SAITO, K., YAMAZAKI, M., SUZUKI, H. & KUSHIRO, T.
866 2016. Onocerin Biosynthesis Requires Two Highly Dedicated Triterpene Cyclases in a Fern Lycopodium
867 clavatum. *ChemBioChem,* 17**,** 288-290.
868 ATHENSTAEDT, K., ZWEYTICK, D., JANDROSITZ, A., KOHLWEIN, S. D. & DAUM, G. 1999. Identification and
869 Characterization of Major Lipid Particle Proteins of the Yeast Saccharomyces cerevisiae. *Journal of*
870 *Bacteriology,* 181**,** 6441-6448.
871 AUGUSTIN, J. M., KUZINA, V., ANDERSEN, S. B. & BAK, S. 2011. Molecular activities, biosynthesis and evolution
872 of triterpenoid saponins. *Phytochemistry,* 72**,** 435-457.
873 BAI, M., XIAO, X.-Y. & PRESTWICH, G. D. 1992. Epoxidation of 2,3-0Xidosqualene to 2,3;22,23-Squalene Dioxide
874 by Squalene Epoxidase. *Biochemical and Biophysical Research Communications,* 185**,** 323-329.
875 BARTON, D. H. R. & OVERTON, K. H. 1955. Triterpenoids. Part XX. The constitution and stereochemistry of a
876 novel tetracyclic triterpenoid. *Journal of the Chemical Society (Resumed)***,** 2639-2652.
877 BENVENISTE, P. 2004. BIOSYNTHESIS AND ACCUMULATION OF STEROLS. *Annual Review of Plant Biology,* 55**,**
878 429-457.
879 BERGER, S. & SICKER, D. 2009. *Classics in Spectroscopy. Isolation and Structure Elucidation of Natural Products,*
880 Weinheim, Wiley-VCH Verlag GmbH & Co. KGaA.
881 BOAR, R. B., COUCHMAN, L. A., JAQUES, A. J. & PERKINS, M. J. 1984. Isolation from Pistacia resins of a bicyclic
882 triterpenoid representing an apparent trapped intermediate of squalene 2,3-epoxide cyclization.
883 *Journal of the American Chemical Society,* 106**,** 2476-2477.
884 COREY, E. J. & RUSSEY, W. E. 1966. Metabolic Fate of 10,11-Dihydrosqualene in Sterol-Producing Rat Liver
885 Homogenate. *Journal of the American Chemical Society,* 88**,** 4751-4752.
886 DAVIS, I. W., LEAVER-FAY, A., CHEN, V. B., BLOCK, J. N., KAPRAL, G. J., WANG, X., MURRAY, L. W., ARENDALL, I. I.
887 I. W. B., SNOEYINK, J., RICHARDSON, J. S. & RICHARDSON, D. C. 2007. MolProbity: all-atom contacts and
888 structure validation for proteins and nucleic acids. *Nucleic Acids Research,* 35**,** W375-W383.
889 ESWAR, N., WEBB, B., MARTI-RENOM, M. A., MADHUSUDHAN, M. S., ERAMIAN, D., SHEN, M.-Y., PIEPER, U. &
890 SALI, A. 2001. Comparative Protein Structure Modeling Using MODELLER. *Current Protocols in Protein*
891 *Science.* John Wiley & Sons, Inc.
892 FIALLOS-JURADO, J., POLLIER, J., MOSES, T., ARENDT, P., BARRIGA-MEDINA, N., MORILLO, E., ARAHANA, V., DE
893 LOURDES TORRES, M., GOOSSENS, A. & LEON-REYES, A. 2016. Saponin determination, expression
894 analysis and functional characterization of saponin biosynthetic genes in Chenopodium quinoa leaves.
895 *Plant Science,* 250**,** 188-197.
896 FIELD, R. B. & HOLMLUND, C. E. 1977. Isolation of 2,3;22,23-dioxidosqualene and 24,25-oxidolanosterol from
897 yeast. *Archives of Biochemistry and Biophysics,* 180**,** 465-471.
898 GACHOTTE, D., ECKSTEIN, J., BARBUCH, R., HUGHES, T., ROBERTS, C. & BARD, M. 2001. A novel gene conserved
899 from yeast to humans is involved in sterol biosynthesis. *Journal of Lipid Research,* 42**,** 150-154.
900 GEU-FLORES, F., NOUR-ELDIN, H. H., NIELSEN, M. T. & HALKIER, B. A. 2007. USER fusion: a rapid and efficient
901 method for simultaneous fusion and cloning of multiple PCR products. *Nucleic Acids Research,* 35**,** e55-
902 e55.

GRABHERR, M. G., HAAS, B. J., YASSOUR, M., LEVIN, J. Z., THOMPSON, D. A., AMIT, I., ADICONIS, X., FAN, L., RAYCHOWDHURY, R., ZENG, Q., CHEN, Z., MAUCELI, E., HACOHEN, N., GNIRKE, A., RHIND, N., DI PALMA, F., BIRREN, B. W., NUSBAUM, C., LINDBLAD-TOH, K., FRIEDMAN, N. & REGEV, A. 2011. Full-length transcriptome assembly from RNA-Seq data without a reference genome. *Nat Biotech,* 29**,** 644-652.

HAYASHI, H., HUANG, P., TAKADA, S., OBINATA, M., INOUE, K., SHIBUYA, M. & EBIZUKA, Y. 2004. Differential Expression of Three Oxidosqualene Cyclase mRNAs in *Glycyrrhiza glabra*. *Biological and Pharmaceutical Bulletin,* 27**,** 1086-1092.

HAYES, S. P. 2012. *Studies into the occurrence of a-onocerin in restharrow.* PhD PhD, The University of Nottingham.

HLASIWETZ, H. 1855. Ueber die Wurzel der Ononis spinosa. *Journal für Praktische Chemie,* 65**,** 419-450.

JONES, D. T., TAYLOR, W. R. & THORNTON, J. M. 1992. The rapid generation of mutation data matrices from protein sequences. *Bioinformatics,* 8**,** 275-282.

KANDUTSCH, A. A., CHEN, H. W. & HEINIGER, H. J. 1978. Biological activity of some oxygenated sterols. *Science,* 201**,** 498.

KHAKIMOV, B., MOTAWIA, M. S., BAK, S. & ENGELSEN, S. B. 2013. The use of trimethylsilyl cyanide derivatization for robust and broad-spectrum high-throughput gas chromatography–mass spectrometry based metabolomics. *Analytical and Bioanalytical Chemistry,* 405**,** 9193-9205.

KRIBII, R., ARRÓ, M., DEL ARCO, A., GONZÁLEZ, V., BALCELLS, L., DELOURME, D., FERRER, A., KARST, F. & BORONAT, A. 1997. Cloning and Characterization of the Arabidopsis Thaliana SQS1 Gene Encoding Squalene Synthase. *European Journal of Biochemistry,* 249**,** 61-69.

KUSHIRO, T., SHIBUYA, M. & EBIZUKA, Y. 1998. β-Amyrin synthase. *European Journal of Biochemistry,* 256**,** 238-244.

LALONDE, S., EHRHARDT, D. W., LOQUÉ, D., CHEN, J., RHEE, S. Y. & FROMMER, W. B. 2008. Molecular and cellular approaches for the detection of protein–protein interactions: latest techniques and current limitations. *The Plant Journal,* 53**,** 610-635.

LAURSEN, T., BORCH, J., KNUDSEN, C., BAVISHI, K., TORTA, F., MARTENS, H. J., SILVESTRO, D., HATZAKIS, N. S., WENK, M. R., DAFFORN, T. R., OLSEN, C. E., MOTAWIA, M. S., HAMBERGER, B., MØLLER, B. L. & BASSARD, J.-E. 2016. Characterization of a dynamic metabolon producing the defense compound dhurrin in sorghum. *Science,* 354**,** 890.

LEBER, R., LANDL, K., ZINSER, E., AHORN, H., SPÖK, A., KOHLWEIN, S. D., TURNOWSKY, F. & DAUM, G. 1998. Dual Localization of Squalene Epoxidase, Erg1p, in Yeast Reflects a Relationship between the Endoplasmic Reticulum and Lipid Particles. *Molecular Biology of the Cell,* 9**,** 375-386.

LODEIRO, S., XIONG, Q., WILSON, W. K., KOLESNIKOVA, M. D., ONAK, C. S. & MATSUDA, S. P. T. 2007. An Oxidosqualene Cyclase Makes Numerous Products by Diverse Mechanisms: A Challenge to Prevailing Concepts of Triterpene Biosynthesis. *Journal of the American Chemical Society,* 129**,** 11213-11222.

MO, C., VALACHOVIC, M., RANDALL, S. K., NICKELS, J. T. & BARD, M. 2002. Protein–protein interactions among C-4 demethylation enzymes involved in yeast sterol biosynthesis. *Proceedings of the National Academy of Sciences,* 99**,** 9739-9744.

MORRIS, G. M., HUEY, R., LINDSTROM, W., SANNER, M. F., BELEW, R. K., GOODSELL, D. S. & OLSON, A. J. 2009. AutoDock4 and AutoDockTools4: Automated docking with selective receptor flexibility. *Journal of Computational Chemistry,* 30**,** 2785-2791.

MOSES, T., POLLIER, J., ALMAGRO, L., BUYST, D., VAN MONTAGU, M., PEDREÑO, M. A., MARTINS, J. C., THEVELEIN, J. M. & GOOSSENS, A. 2014. Combinatorial biosynthesis of sapogenins and saponins in Saccharomyces cerevisiae using a C-16α hydroxylase from Bupleurum falcatum. *Proceedings of the National Academy of Sciences,* 111**,** 1634-1639.

NAGUMO, A., KAMEI, T., SAKAKIBARA, J. & ONO, T. 1995. Purification and characterization of recombinant squalene epoxidase. *Journal of Lipid Research,* 36**,** 1489-1497.

OLIARO-BOSSO, S., CARON, G., TARAMINO, S., ERMONDI, G., VIOLA, F. & BALLIANO, G. 2011. Characterization of the Channel Constriction Allowing the Access of the Substrate to the Active Site of Yeast Oxidosqualene Cyclase. *PLoS ONE,* 6**,** e22134.

OLIARO-BOSSO, S., SCHULZ-GASCH, T., BALLIANO, G. & VIOLA, F. 2005. Access of the Substrate to the Active Site of Yeast Oxidosqualene Cyclase: An Inhibition and Site-Directed Mutagenesis Approach. *ChemBioChem,* 6**,** 2221-2228.

PETTERSEN, E. F., GODDARD, T. D., HUANG, C. C., COUCH, G. S., GREENBLATT, D. M., MENG, E. C. & FERRIN, T. E. 2004. UCSF Chimera—A visualization system for exploratory research and analysis. *Journal of Computational Chemistry,* 25**,** 1605-1612.

PINA, E. S., SILVA, D. B., TEIXEIRA, S. P., COPPEDE, J. S., FURLAN, M., FRANÇA, S. C., LOPES, N. P., PEREIRA, A. M. S. & LOPES, A. A. 2016. Mevalonate-derived quinonemethide triterpenoid from in vitro roots of Peritassa laevigata and their localization in root tissue by MALDI imaging. *Scientific Reports,* 6**,** 22627.

RASBERY, J. M., SHAN, H., LECLAIR, R. J., NORMAN, M., MATSUDA, S. P. T. & BARTEL, B. 2007. Arabidopsis thaliana Squalene Epoxidase 1 Is Essential for Root and Seed Development. *Journal of Biological Chemistry,* 282**,** 17002-17013.

ROWAN, M. G. & DEAN, P. D. G. 1972. α-Onocerin and sterol content of twelve species of Ononis. *Phytochemistry,* 11**,** 3263-3265.

ROWAN, M. G., DEAN, P. D. G. & GOODWIN, T. W. 1971. The enzymic conversion of squalene, 2(3),22(23)-diepoxide to α-onocerin by a cell-free extract of Ononis spinosa. *FEBS Letters,* 12**,** 229-232.

SAINSBURY, F. & LOMONOSSOFF, G. P. 2008. Extremely High-Level and Rapid Transient Protein Production in Plants without the Use of Viral Replication. *Plant Physiology,* 148**,** 1212-1218.

SAWAI, S., SHINDO, T., SATO, S., KANEKO, T., TABATA, S., AYABE, S.-I. & AOKI, T. 2006. Functional and structural analysis of genes encoding oxidosqualene cyclases of Lotus japonicus. *Plant Science,* 170**,** 247-257.

SCHAEFER, P. C., DE REINACH, F. & OURISSON, G. 1970. The Conversion of Parkeol into its 24,25-Epoxide by Tissue Cultures of Nicotiana tabacum. *European Journal of Biochemistry,* 14**,** 284-288.

SCHNEIDER, C. A., RASBAND, W. S. & ELICEIRI, K. W. 2012. NIH Image to ImageJ: 25 years of image analysis. *Nat Meth,* 9**,** 671-675.

SPENCER, T. A. 1994. The squalene dioxide pathway of steroid biosynthesis. *Accounts of Chemical Research,* 27**,** 83-90.

SUZUKI, H., ACHNINE, L., XU, R., MATSUDA, S. P. T. & DIXON, R. A. 2002. A genomics approach to the early stages of triterpene saponin biosynthesis in Medicago truncatula. *The Plant Journal,* 32**,** 1033-1048.

TAMURA, K., STECHER, G., PETERSON, D., FILIPSKI, A. & KUMAR, S. 2013. MEGA6: Molecular Evolutionary Genetics Analysis Version 6.0. *Molecular Biology and Evolution,* 30**,** 2725-2729.

THOMA, R., SCHULZ-GASCH, T., D'ARCY, B., BENZ, J., AEBI, J., DEHMLOW, H., HENNIG, M., STIHLE, M. & RUF, A. 2004. Insight into steroid scaffold formation from the structure of human oxidosqualene cyclase. *Nature,* 432**,** 118-122.

TIAN, B.-X. & ERIKSSON, L. A. 2012. Catalytic Mechanism and Product Specificity of Oxidosqualene-Lanosterol Cyclase: A QM/MM Study. *The Journal of Physical Chemistry B,* 116**,** 13857-13862.

TURINI, F. G., BRÄUCHLER, C. & HEUBL, G. 2010. Phylogenetic relationships and evolution of morphological characters in Ononis L. (Fabaceae). *Taxon,* 59**,** 1077-1090.

VAN DER FITS, L., DEAKIN, E. A., HOGE, J. H. C. & MEMELINK, J. 2000. The ternary transformation system: constitutive virG on a compatible plasmid dramatically increases Agrobacterium-mediated plant transformation. *Plant Molecular Biology,* 43**,** 495-502.

994 VAN TAMELEN, E. E. & HEYS, J. R. 1975. Enzymic epoxidation of squalene variants. *Journal of the American*
995 *Chemical Society,* 97**,** 1252-1253.
996 VAN TAMELEN, E. E., LEOPOLD, E. J., MARSON, S. A. & WAESPE, H. R. 1982. Action of 2,3-oxidosqualene
997 lanosterol cyclase on 15'-nor-18,19-dihydro-2,3-oxidosqualene. *Journal of the American Chemical*
998 *Society,* 104**,** 6479-6480.
999 WHELAN, J. A., RUSSELL, N. B. & WHELAN, M. A. 2003. A method for the absolute quantification of cDNA using
1000 real-time PCR. *Journal of Immunological Methods,* 278**,** 261-269.
1001 WIEDERSTEIN, M. & SIPPL, M. J. 2007. ProSA-web: interactive web service for the recognition of errors in three-
1002 dimensional structures of proteins. *Nucleic Acids Research,* 35**,** W407-W410.
1003 WOJCIECHOWSKI, M. F., LAVIN, M. & SANDERSON, M. J. 2004. A phylogeny of legumes (Leguminosae) based on
1004 analysis of the plastid matK gene resolves many well-supported subclades within the family. *American*
1005 *Journal of Botany,* 91**,** 1846-1862.
1006 WU, T.-K., WANG, T.-T., CHANG, C.-H., LIU, Y.-T. & SHIE, W.-S. 2008. Importance of Saccharomyces cerevisiae
1007 Oxidosqualene-Lanosterol Cyclase Tyrosine 707 Residue for Chair-Boat Bicyclic Ring Formation and
1008 Deprotonation Reactions. *Organic Letters,* 10**,** 4959-4962.
1009 XU, R., FAZIO, G. C. & MATSUDA, S. P. T. 2004. On the origins of triterpenoid skeletal diversity. *Phytochemistry,*
1010 65**,** 261-291.

1011

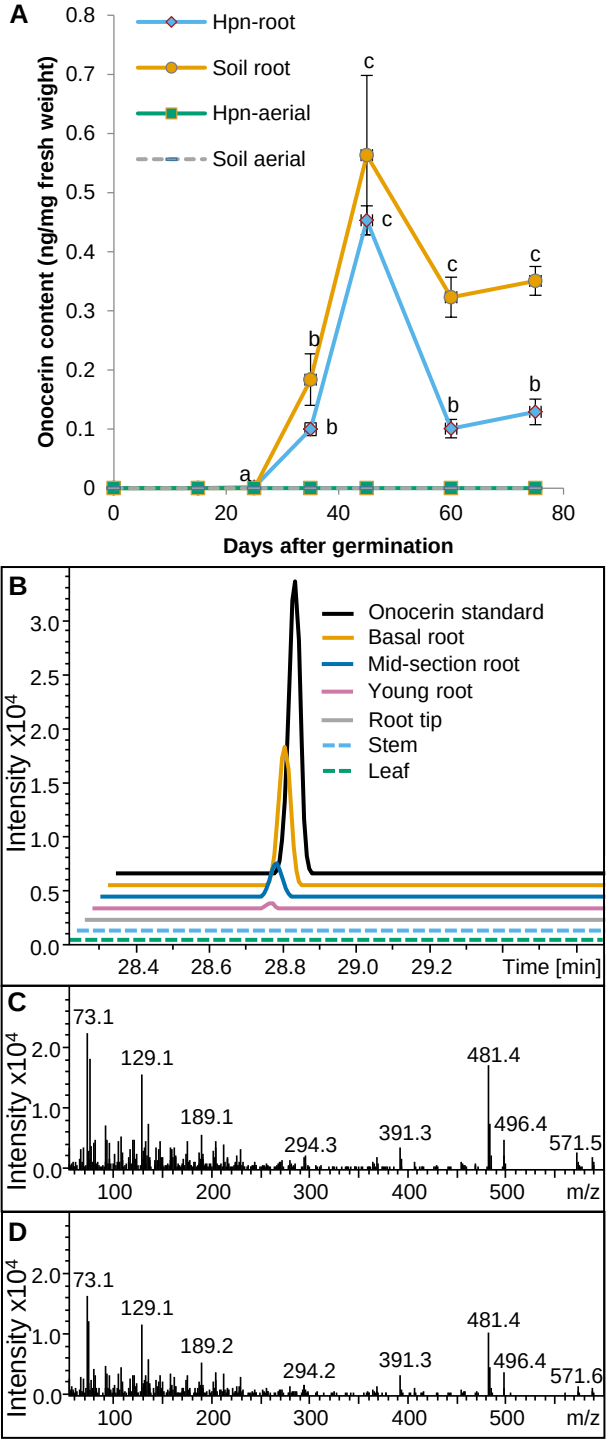

Figure 1. α-Onocerin content varies throughout plant growth and across the root length. A, Time course of α-onocerin accumulation in root and aerial tissues (fresh weight) of *O. spinosa* plants grown in either soil or hydroponics (Hpn) system. B, Extracted ion chromatograms (480-482m/z) of *O. spinosa* root sections, stem and leaf tissues. C, Mass spectrum of derivatized α-onocerin standard. D, Representative mass spectrum of α-onocerin peak in derivatized extracts from root sections. Values represent means (±standard error) from three biological replicates for each time point, letters indicate significant differences determined by ANOVA/post-hoc Tukey's HSD test at P<0.05.

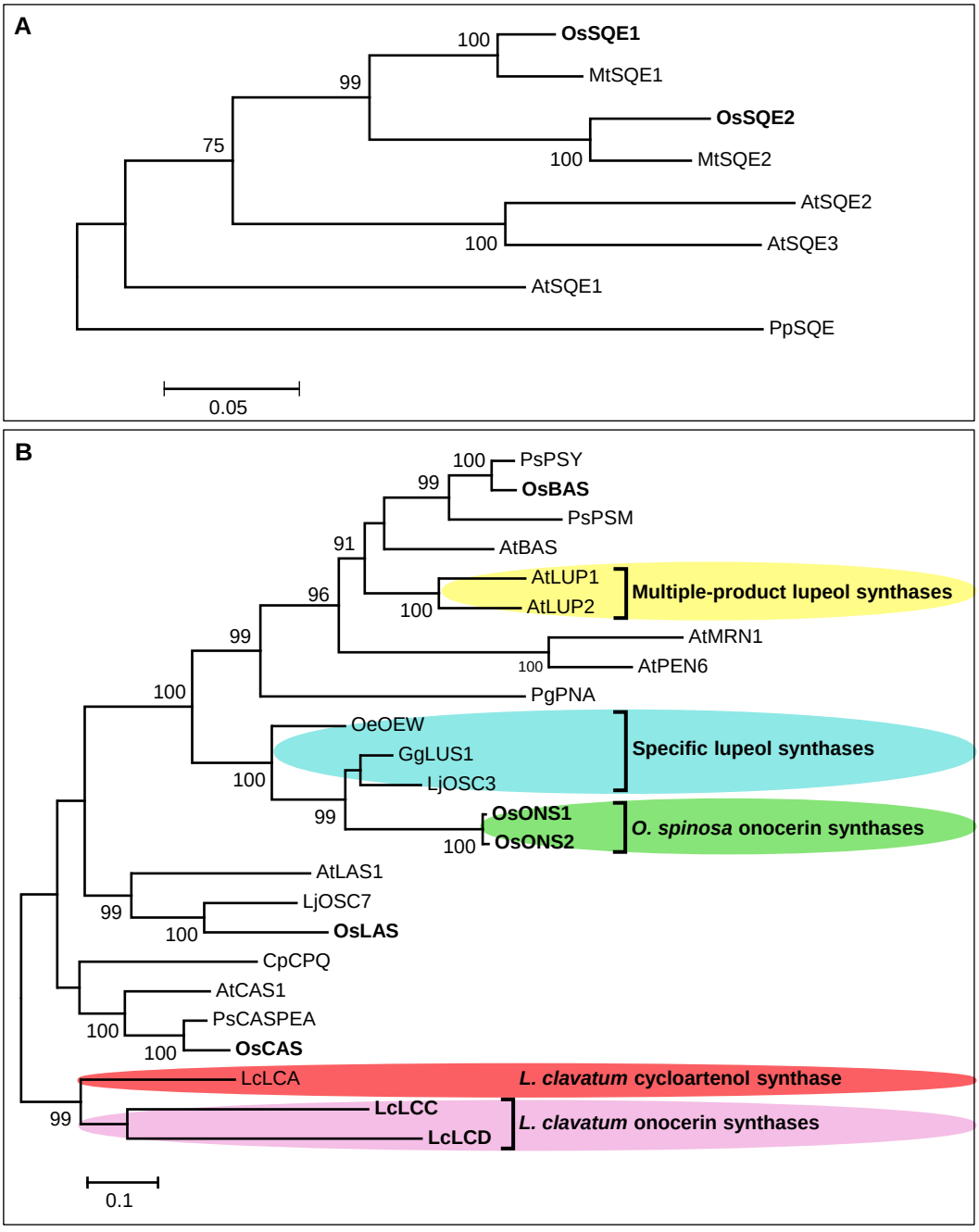

Figure 2. Phylogenetic analysis suggests that the α-onocerin pathway genes in *O. spinosa* and *L. clavatum* are distantly related and arise from convergent evolution. A, Maximum-likelihood tree was constructed on deduced amino acid sequences of eight SQEs aligned by CLUSTALW spanning 496 positions using the MEGA6 program. Statistical significance of each node was tested by the bootstrap method using 1,000 iterations. Representative names: OsSQE1- *Ononis spinosa* squalene epoxidase 1, OsSQE2- *Ononis spinosa* squalene epoxidase 2, MtSQE1- *Medicago truncatula* mRNA for squalene monooxygenase 1, MtSQE2- *Medicago truncatula* mRNA for squalene monooxygenase 2, AtSQE1- *Arabidopsis thaliana* squalene epoxidase 1, AtSQE3- *Arabidopsis thaliana* squalene epoxidase 2, AtSQE3- *Arabidopsis thaliana* squalene epoxidase 3, PpSQE- *Physcomitrella patens* squalene epoxidase.

B, Maximum-likelihood tree was constructed on deduced amino acid sequences 24 OSCs with known product profiles aligned by CLUSTALW spanning 730 positions using the MEGA6 program. Statistical significance of each node was tested by the bootstrap method using 1,000 iterations. Bold letters represent genes from *O. spinosa* and *L. clavatum*. Representative names: OsONS1- *Ononis spinosa* Onocerin synthase 1, OsONS2- *Ononis spinosa* Onocerin synthase 2, OsBAS- *Ononis spinosa* putative β-amyrin synthase, OsCAS- *Ononis spinosa* putative Cycloartenol synthase, OsLAS- *Ononis spinosa* putative Lanosterol synthase, PsCASPEA- (*Pisum sativum* cycloartenol synthase, PsOSCPSY- *Pisum sativum* β-amyrin synthase, PsOSCPSM- *Pisum sativum* mixed-amyrin synthase, MtBAS- *Medicago truncatula* β-amyrin synthase, AtLUP1- *Arabidopsis thaliana* lupeol synthase 1, AtLUP2- *Arabidopsis thaliana* lupeol synthase 2, AtPEN6- *Arabidopsis thaliana seco*- β-amyrin synthase, AtMRN1- *Arabidopsis thaliana* Marneral synthase, AtBAS- *Arabidopsis thaliana* β-amyrin synthase, AtCAS1- *Arabidopsis thaliana* cycloartenol synthase, AtLAS1- *Arabidopsis thaliana* Lanosterol synthase, PgPNA- *Panax ginseng* dammarenediol-II synthase, LcLCA- *Lycopodium clavatum* cycloartenol synthase, LcLCC- *Lycopodium clavatum* pre-α-onocerin synthase, LcLCD- *Lycopodium clavatum* onocerin synthase, OeOEW- *Olea europaea* lupeol synthase, GgLUS1- *Glycyrrhiza glabra* lupeol synthase, LjOSC3- *Lotus japonicus* lupeol synthase, LjOSC7- *Lotus japonicus* lanosterol synthase, CpCPQ- *Cucurbita pepo* cucurbitadienol synthase.

GenBank ID numbers for each nucleotide sequence of OSCs and SQEs are given in the experimental procedures section.

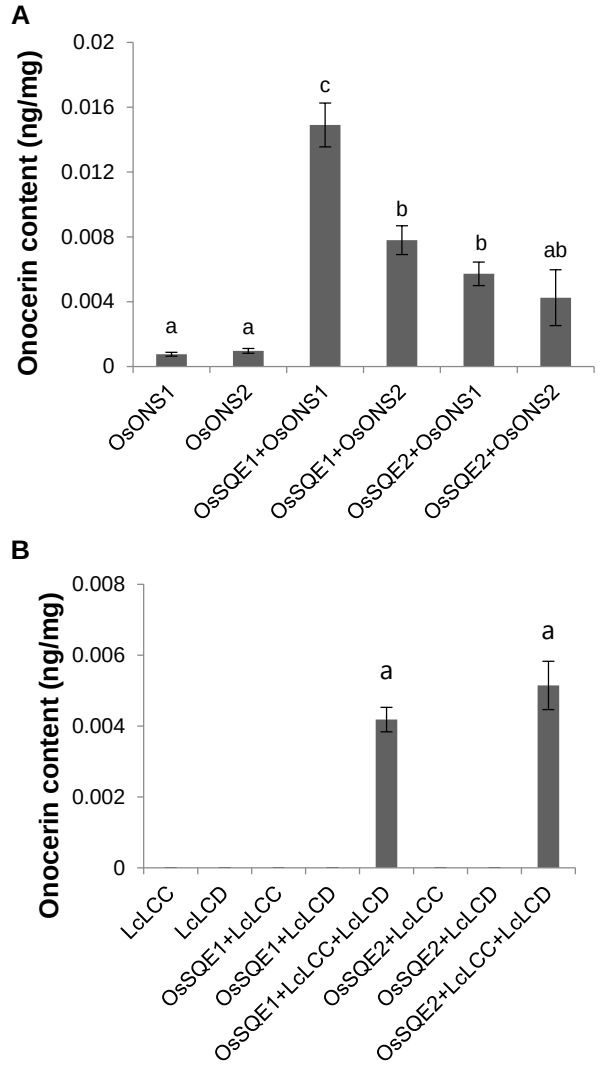

Figure 3. α-Onocerin biosynthesis in *O. spinosa* is biochemically different from that of *L. clavatum*.

A, α-Onocerin content of *N. benthamiana* leaves transiently transformed with *OSCs* and *SQEs* of *O. spinosa*. B, α-Onocerin content of *N. benthamiana* leaves transiently transformed with α-onocerin synthases of *L. clavatum* co-expressed with *SQEs* of *O. spinosa*. C, Total ion chromatogram showing production of α-onocerin in yeast strain GIL77 transformed with *OsONS1* of *O. spinosa*. Values represent means (±standard error) from three biological replicates, letters indicate significant differences determined by ANOVA/post-hoc Tukey's HSD test at $P<0.05$.

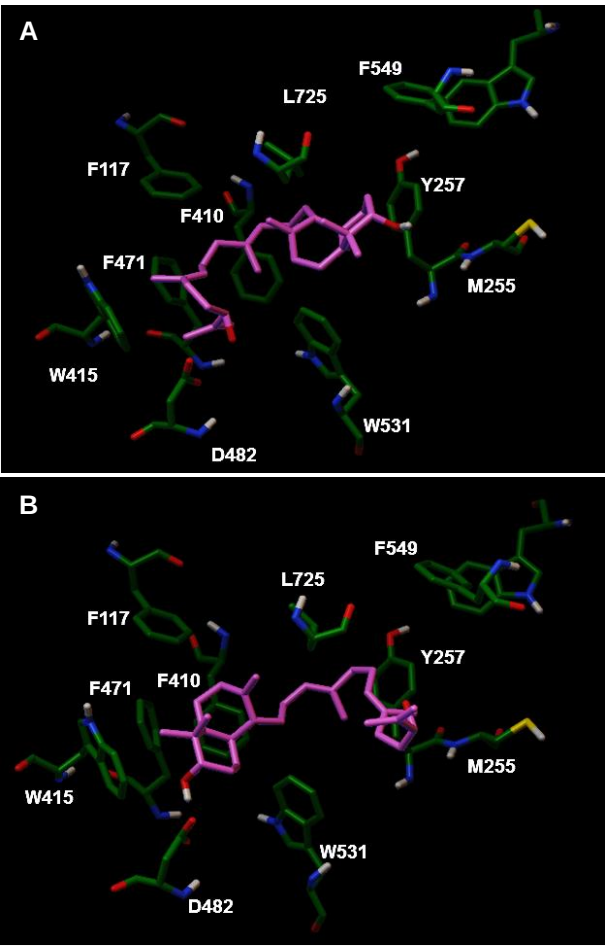

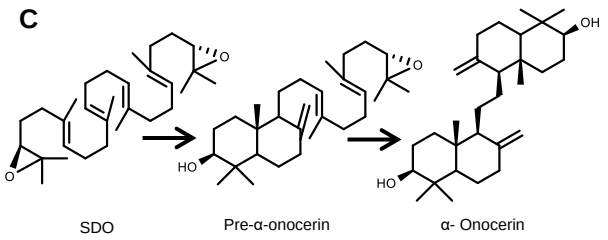

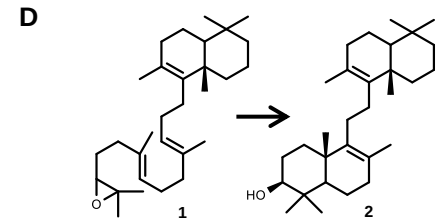

Figure 4. Docking simulations of OsONS1 homology model shows pre-α-onocerin can dock from both ends to the catalytic aspartate residue, D482. Color coding: Pink-Carbon atoms of pre-α-onocerin, green: Carbon atoms in amino acid residues of OsONS1 homology model, red: oxygen atoms, blue- nitrogen atoms, white- hydrogen atoms, yellow- sulfur atoms. A, Epoxide end of pre-α-onocerin forming hydrogen bond with catalytic aspartate D482 in active site of OsONS1-homology model. B, Hydroxyl group from cyclized end of pre-α-onocerin forming hydrogen bond with catalytic aspartate D482 in active site of OsONS1-homology model. C, Steps of α-onocerin biosynthetic pathway. D, Demonstrated cyclization reaction by rabbit microsomes. Compound **1:** 3-((3*E*,7*E*)-3,7-dimethyl-10-((8a*S*)-2,5,5,8a-tetramethyl-3,4,4a,5,6,7,8,8a-octahydronaphthalen-1-yl)deca-3,7-dien-1-yl)-2,2-dimethyloxirane and compound **2**: 8,14-*seco*-gammacera-7,14-diene-3-ol.

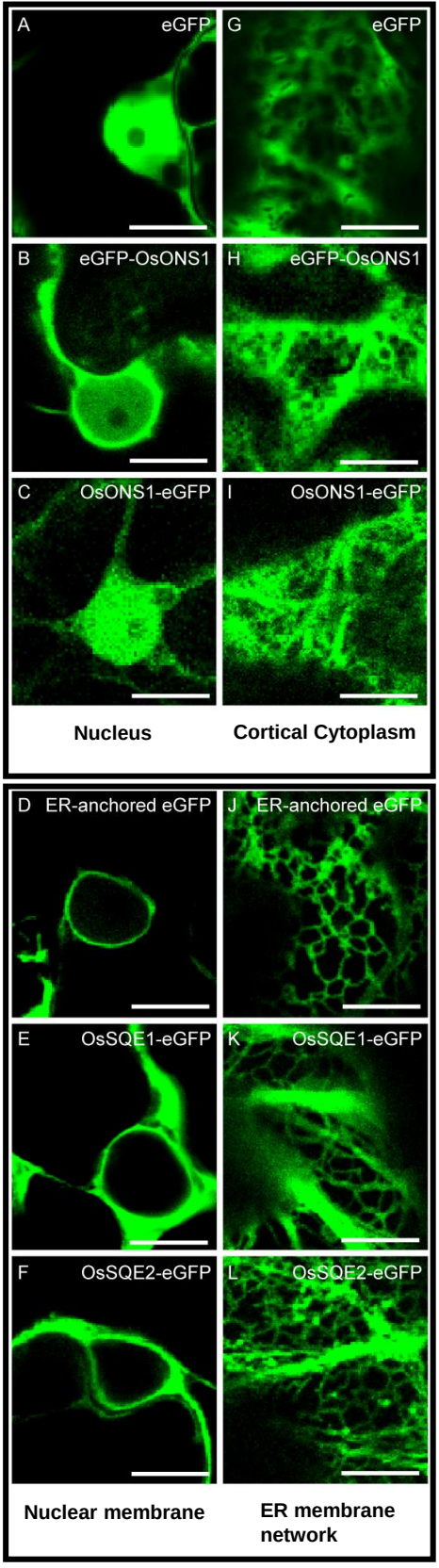

Figure 5. OsONS1 is localizes in the cytoplasm, while OsSQEs are restricted to the ER membrane as visualized by confocal microscopy of *N. benthamiana* epidermal leaves. Confocal Laser Scanning Microscopy (CLSM) images were collected 3 days after agroinfiltration of *N. benthamiana* leaves. Representative confocal images of the nucleus (A-F) and parietal cell space (G-L) of leaves expressing eGFP-tagged target proteins are shown. Soluble enzymes may permeate through the nuclear pores and be found inside the nucleus (A-C) and fill out the cytoplasm around cortical ER (G-I). ER proteins are restrained to nuclear membranes (D-F) and to a characteristic ER membrane network (J-L). Due to turgescent vacuole pushing the cytoplasm and ER near the plasma membrane, well defined ER network and diffused cytoplasmic patterns may be visualized when observing the cortical space in epidermal cells of *N. benthamiana* leaves.
Scale bars = 10 µm.

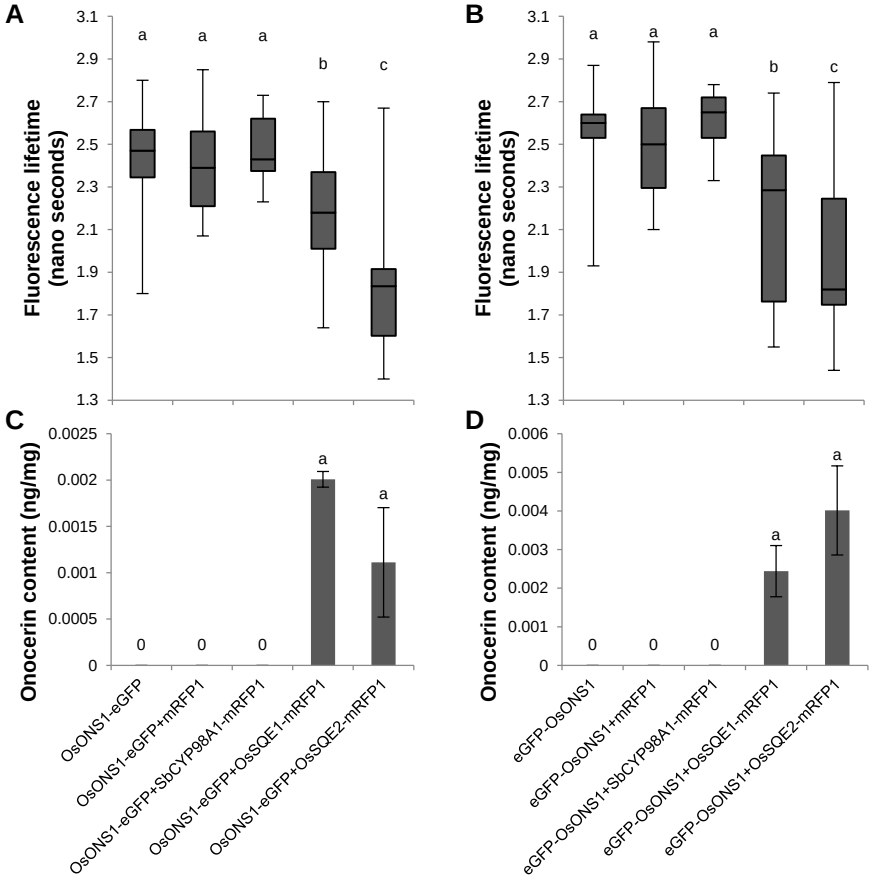

Figure 6. OsONS1 interacts with both OsSQE1 and OsSQE2. A, FLIM values for *OsONS1* tagged with *eGFP* on the C-terminal co-expressed with several *mRFP1* fused constructs in transiently transformed *N. benthamiana* leaves. B, FLIM values for *OsONS1* tagged with *eGFP* on the N-terminal co-expressed with several *mRFP1* tagged constructs in transiently transformed *N. benthamiana* leaves. C, α-Onocerin content of *N. benthamiana* leaves transiently transformed with *OsONS1-eGFP* co-expressed with several *mRFP1* tagged constructs. D, α-Onocerin content of *N. benthamiana* leaves transiently transformed with *eGFP-OsONS1* co-expressed with several *mRFP1* tagged constructs. For figures A and B, letters indicate significant differences determined by ANOVA/post-hoc Scheffe's method at P<0.05. For figure C and D, Values represent means (±standard error) from three biological replicates, letters indicate significant differences determined by ANOVA/post-hoc Tukey's HSD test at P<0.05.

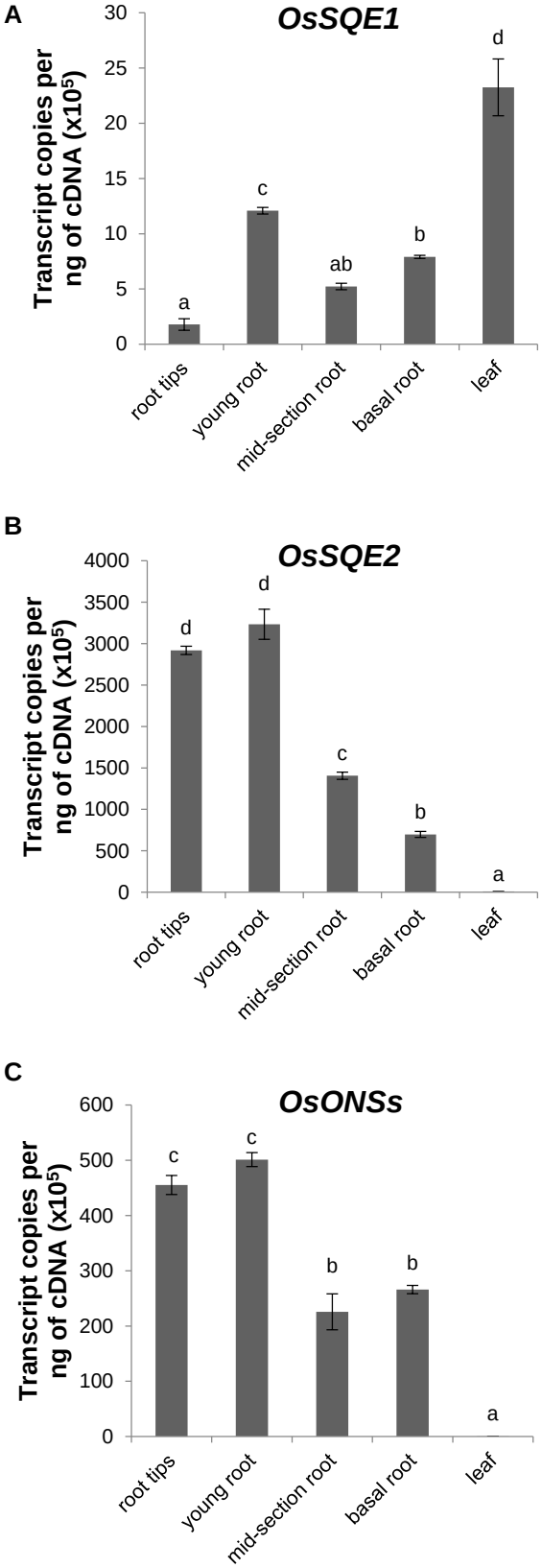

Figure 7. *OsSQE2* and *OsONSs* co-express across root sections and leaves of *O. spinosa*. A, absolute quantification of *OsSQE1* number of transcripts in different tissues of *O. spinosa*. B, absolute quantification of *OsSQE2* number of transcripts in different tissues of *O. spinosa*. C, absolute quantification of *OsONSs* number of transcripts in different tissues of *O. spinosa*. Reverse Transcription-quantitative PCR was performed on RNA extracted from the pooled tissues of 5 plants. Values represent mean (±standard error) from three different pooling per tissue, letters indicate significant differences determined by ANOVA/post-hoc Tukey's HSD test at $P<0.05$.

Parsed Citations

2015. Correction. The Plant Journal, 83, 752-752.

ABE, I. 2014. The Oxidosqualene Cyclases: One Substrate, Diverse Products. Natural Products. John Wiley & Sons, Inc.
Pubmed: Author and Title
CrossRef: Author and Title
Google Scholar: Author Only Title Only Author and Title

AGETA, H., IWATA, K. & OOTAKE, Y. 1962. Isolation of α-onocerin from Lycopodium clavatum INN. CHEMICAL & PHARMACEUTICAL BULLETIN, 10, 637-637.
Pubmed: Author and Title
CrossRef: Author and Title
Google Scholar: Author Only Title Only Author and Title

ARAKI, T., SAGA, Y., MARUGAMI, M., OTAKA, J., ARAYA, H., SAITO, K., YAMAZAKI, M., SUZUKI, H. & KUSHIRO, T. 2016. Onocerin Biosynthesis Requires Two Highly Dedicated Triterpene Cyclases in a Fern Lycopodium clavatum. ChemBioChem, 17, 288-290.
Pubmed: Author and Title
CrossRef: Author and Title
Google Scholar: Author Only Title Only Author and Title

ATHENSTAEDT, K., ZWEYTICK, D., JANDROSITZ, A., KOHLWEIN, S. D. & DAUM, G. 1999. Identification and Characterization of Major Lipid Particle Proteins of the Yeast Saccharomyces cerevisiae. Journal of Bacteriology, 181, 6441-6448.
Pubmed: Author and Title
CrossRef: Author and Title
Google Scholar: Author Only Title Only Author and Title

AUGUSTIN, J. M., KUZINA, V., ANDERSEN, S. B. & BAK, S. 2011. Molecular activities, biosynthesis and evolution of triterpenoid saponins. Phytochemistry, 72, 435-457.
Pubmed: Author and Title
CrossRef: Author and Title
Google Scholar: Author Only Title Only Author and Title

BAI, M., XIAO, X.-Y. & PRESTWICH, G. D. 1992. Epoxidation of 2,3-0Xidosqualene to 2,3;22,23-Squalene Dioxide by Squalene Epoxidase. Biochemical and Biophysical Research Communications, 185, 323-329.
Pubmed: Author and Title
CrossRef: Author and Title
Google Scholar: Author Only Title Only Author and Title

BARTON, D. H. R. & OVERTON, K. H. 1955. Triterpenoids. Part XX. The constitution and stereochemistry of a novel tetracyclic triterpenoid. Journal of the Chemical Society (Resumed), 2639-2652.
Pubmed: Author and Title
CrossRef: Author and Title
Google Scholar: Author Only Title Only Author and Title

BENVENISTE, P. 2004. BIOSYNTHESIS AND ACCUMULATION OF STEROLS. Annual Review of Plant Biology, 55, 429-457.
Pubmed: Author and Title
CrossRef: Author and Title
Google Scholar: Author Only Title Only Author and Title

BERGER, S. & SICKER, D. 2009. Classics in Spectroscopy. Isolation and Structure Elucidation of Natural Products, Weinheim, Wiley-VCH Verlag GmbH & Co. KGaA.
Pubmed: Author and Title
CrossRef: Author and Title
Google Scholar: Author Only Title Only Author and Title

BOAR, R. B., COUCHMAN, L. A., JAQUES, A. J. & PERKINS, M. J. 1984. Isolation from Pistacia resins of a bicyclic triterpenoid representing an apparent trapped intermediate of squalene 2,3-epoxide cyclization. Journal of the American Chemical Society, 106, 2476-2477.
Pubmed: Author and Title
CrossRef: Author and Title
Google Scholar: Author Only Title Only Author and Title

COREY, E. J. & RUSSEY, W. E. 1966. Metabolic Fate of 10,11-Dihydrosqualene in Sterol-Producing Rat Liver Homogenate. Journal of the American Chemical Society, 88, 4751-4752.
Pubmed: Author and Title
CrossRef: Author and Title
Google Scholar: Author Only Title Only Author and Title

DAVIS, I. W., LEAVER-FAY, A., CHEN, V. B., BLOCK, J. N., KAPRAL, G. J., WANG, X., MURRAY, L. W., ARENDALL, I. I. I. W. B., SNOEYINK, J., RICHARDSON, J. S. & RICHARDSON, D. C. 2007. MolProbity: all-atom contacts and structure validation for proteins and nucleic acids. Nucleic Acids Research, 35, W375-W383.
Pubmed: Author and Title
CrossRef: Author and Title

Google Scholar: Author Only Title Only Author and Title

ESWAR, N., WEBB, B., MARTI-RENOM, M. A., MADHUSUDHAN, M. S., ERAMIAN, D., SHEN, M.-Y., PIEPER, U. & SALI, A. 2001. Comparative Protein Structure Modeling Using MODELLER. Current Protocols in Protein Science. John Wiley & Sons, Inc.
Pubmed: Author and Title
CrossRef: Author and Title
Google Scholar: Author Only Title Only Author and Title

FIALLOS-JURADO, J., POLLIER, J., MOSES, T., ARENDT, P., BARRIGA-MEDINA, N., MORILLO, E., ARAHANA, V., DE LOURDES TORRES, M., GOOSSENS, A. & LEON-REYES, A. 2016. Saponin determination, expression analysis and functional characterization of saponin biosynthetic genes in Chenopodium quinoa leaves. Plant Science, 250, 188-197.
Pubmed: Author and Title
CrossRef: Author and Title
Google Scholar: Author Only Title Only Author and Title

FIELD, R. B. & HOLMLUND, C. E. 1977. Isolation of 2,3;22,23-dioxidosqualene and 24,25-oxidolanosterol from yeast. Archives of Biochemistry and Biophysics, 180, 465-471.
Pubmed: Author and Title
CrossRef: Author and Title
Google Scholar: Author Only Title Only Author and Title

GACHOTTE, D., ECKSTEIN, J., BARBUCH, R., HUGHES, T., ROBERTS, C. & BARD, M. 2001. A novel gene conserved from yeast to humans is involved in sterol biosynthesis. Journal of Lipid Research, 42, 150-154.
Pubmed: Author and Title
CrossRef: Author and Title
Google Scholar: Author Only Title Only Author and Title

GEU-FLORES, F., NOUR-ELDIN, H. H., NIELSEN, M. T. & HALKIER, B. A. 2007. USER fusion: a rapid and efficient method for simultaneous fusion and cloning of multiple PCR products. Nucleic Acids Research, 35, e55-e55.
Pubmed: Author and Title
CrossRef: Author and Title
Google Scholar: Author Only Title Only Author and Title

GRABHERR, M. G., HAAS, B. J., YASSOUR, M., LEVIN, J. Z., THOMPSON, D. A., AMIT, I., ADICONIS, X., FAN, L., RAYCHOWDHURY, R., ZENG, Q., CHEN, Z., MAUCELI, E., HACOHEN, N., GNIRKE, A., RHIND, N., DI PALMA, F., BIRREN, B. W., NUSBAUM, C., LINDBLAD-TOH, K., FRIEDMAN, N. & REGEV, A. 2011. Full-length transcriptome assembly from RNA-Seq data without a reference genome. Nat Biotech, 29, 644-652.
Pubmed: Author and Title
CrossRef: Author and Title
Google Scholar: Author Only Title Only Author and Title

HAYASHI, H., HUANG, P., TAKADA, S., OBINATA, M., INOUE, K., SHIBUYA, M. & EBIZUKA, Y. 2004. Differential Expression of Three Oxidosqualene Cyclase mRNAs in Glycyrrhiza glabra. Biological and Pharmaceutical Bulletin, 27, 1086-1092.
Pubmed: Author and Title
CrossRef: Author and Title
Google Scholar: Author Only Title Only Author and Title

HAYES, S. P. 2012. Studies into the occurrence of a-onocerin in restharrow. PhD PhD, The University of Nottingham.
Pubmed: Author and Title
CrossRef: Author and Title
Google Scholar: Author Only Title Only Author and Title

HLASIWETZ, H. 1855. Ueber die Wurzel der Ononis spinosa. Journal für Praktische Chemie, 65, 419-450.
Pubmed: Author and Title
CrossRef: Author and Title
Google Scholar: Author Only Title Only Author and Title

JONES, D. T., TAYLOR, W. R. & THORNTON, J. M. 1992. The rapid generation of mutation data matrices from protein sequences. Bioinformatics, 8, 275-282.
Pubmed: Author and Title
CrossRef: Author and Title
Google Scholar: Author Only Title Only Author and Title

KANDUTSCH, A. A., CHEN, H. W. & HEINIGER, H. J. 1978. Biological activity of some oxygenated sterols. Science, 201, 498.
Pubmed: Author and Title
CrossRef: Author and Title
Google Scholar: Author Only Title Only Author and Title

KHAKIMOV, B., MOTAWIA, M. S., BAK, S. & ENGELSEN, S. B. 2013. The use of trimethylsilyl cyanide derivatization for robust and broad-spectrum high-throughput gas chromatography–mass spectrometry based metabolomics. Analytical and Bioanalytical Chemistry, 405, 9193-9205.
Pubmed: Author and Title
CrossRef: Author and Title
Google Scholar: Author Only Title Only Author and Title

KRIBII, R., ARRÓ, M., DEL ARCO, A., GONZÁLEZ, V., BALCELLS, L., DELOURME, D., FERRER, A., KARST, F. & BORONAT, A. 1997. Cloning and Characterization of the Arabidopsis Thaliana SQS1 Gene Encoding Squalene Synthase. European Journal of Biochemistry, 249, 61-69.
Pubmed: Author and Title
CrossRef: Author and Title
Google Scholar: Author Only Title Only Author and Title

KUSHIRO, T., SHIBUYA, M. & EBIZUKA, Y. 1998. β-Amyrin synthase. European Journal of Biochemistry, 256, 238-244.
Pubmed: Author and Title
CrossRef: Author and Title
Google Scholar: Author Only Title Only Author and Title

LALONDE, S., EHRHARDT, D. W., LOQUÉ, D., CHEN, J., RHEE, S. Y. & FROMMER, W. B. 2008. Molecular and cellular approaches for the detection of protein–protein interactions: latest techniques and current limitations. The Plant Journal, 53, 610-635.
Pubmed: Author and Title
CrossRef: Author and Title
Google Scholar: Author Only Title Only Author and Title

LAURSEN, T., BORCH, J., KNUDSEN, C., BAVISHI, K., TORTA, F., MARTENS, H. J., SILVESTRO, D., HATZAKIS, N. S., WENK, M. R., DAFFORN, T. R., OLSEN, C. E., MOTAWIA, M. S., HAMBERGER, B., MØLLER, B. L. & BASSARD, J.-E. 2016. Characterization of a dynamic metabolon producing the defense compound dhurrin in sorghum. Science, 354, 890.
Pubmed: Author and Title
CrossRef: Author and Title
Google Scholar: Author Only Title Only Author and Title

LEBER, R., LANDL, K., ZINSER, E., AHORN, H., SPÖK, A., KOHLWEIN, S. D., TURNOWSKY, F. & DAUM, G. 1998. Dual Localization of Squalene Epoxidase, Erg1p, in Yeast Reflects a Relationship between the Endoplasmic Reticulum and Lipid Particles. Molecular Biology of the Cell, 9, 375-386.
Pubmed: Author and Title
CrossRef: Author and Title
Google Scholar: Author Only Title Only Author and Title

LODEIRO, S., XIONG, Q., WILSON, W. K., KOLESNIKOVA, M. D., ONAK, C. S. & MATSUDA, S. P. T. 2007. An Oxidosqualene Cyclase Makes Numerous Products by Diverse Mechanisms: A Challenge to Prevailing Concepts of Triterpene Biosynthesis. Journal of the American Chemical Society, 129, 11213-11222.
Pubmed: Author and Title
CrossRef: Author and Title
Google Scholar: Author Only Title Only Author and Title

MO, C., VALACHOVIC, M., RANDALL, S. K., NICKELS, J. T. & BARD, M. 2002. Protein–protein interactions among C-4 demethylation enzymes involved in yeast sterol biosynthesis. Proceedings of the National Academy of Sciences, 99, 9739-9744.
Pubmed: Author and Title
CrossRef: Author and Title
Google Scholar: Author Only Title Only Author and Title

MORRIS, G. M., HUEY, R., LINDSTROM, W., SANNER, M. F., BELEW, R. K., GOODSELL, D. S. & OLSON, A. J. 2009. AutoDock4 and AutoDockTools4: Automated docking with selective receptor flexibility. Journal of Computational Chemistry, 30, 2785-2791.
Pubmed: Author and Title
CrossRef: Author and Title
Google Scholar: Author Only Title Only Author and Title

MOSES, T., POLLIER, J., ALMAGRO, L., BUYST, D., VAN MONTAGU, M., PEDREÑO, M. A., MARTINS, J. C., THEVELEIN, J. M. & GOOSSENS, A. 2014. Combinatorial biosynthesis of sapogenins and saponins in Saccharomyces cerevisiae using a C-16α hydroxylase from Bupleurum falcatum. Proceedings of the National Academy of Sciences, 111, 1634-1639.
Pubmed: Author and Title
CrossRef: Author and Title
Google Scholar: Author Only Title Only Author and Title

NAGUMO, A., KAMEI, T., SAKAKIBARA, J. & ONO, T. 1995. Purification and characterization of recombinant squalene epoxidase. Journal of Lipid Research, 36, 1489-1497.
Pubmed: Author and Title
CrossRef: Author and Title
Google Scholar: Author Only Title Only Author and Title

OLIARO-BOSSO, S., CARON, G., TARAMINO, S., ERMONDI, G., VIOLA, F. & BALLIANO, G. 2011. Characterization of the Channel Constriction Allowing the Access of the Substrate to the Active Site of Yeast Oxidosqualene Cyclase. PLoS ONE, 6, e22134.
Pubmed: Author and Title
CrossRef: Author and Title
Google Scholar: Author Only Title Only Author and Title

OLIARO-BOSSO, S., SCHULZ-GASCH, T., BALLIANO, G. & VIOLA, F. 2005. Access of the Substrate to the Active Site of Yeast Oxidosqualene Cyclase: An Inhibition and Site-Directed Mutagenesis Approach. ChemBioChem, 6, 2221-2228.
Pubmed: Author and Title
CrossRef: Author and Title
Google Scholar: Author Only Title Only Author and Title

PETTERSEN, E. F., GODDARD, T. D., HUANG, C. C., COUCH, G. S., GREENBLATT, D. M., MENG, E. C. & FERRIN, T. E. 2004. UCSF Chimera—A visualization system for exploratory research and analysis. Journal of Computational Chemistry, 25, 1605-1612.
Pubmed: Author and Title
CrossRef: Author and Title
Google Scholar: Author Only Title Only Author and Title

PINA, E. S., SILVA, D. B., TEIXEIRA, S. P., COPPEDE, J. S., FURLAN, M., FRANÇA, S. C., LOPES, N. P., PEREIRA, A. M. S. & LOPES, A. A. 2016. Mevalonate-derived quinonemethide triterpenoid from in vitro roots of Peritassa laevigata and their localization in root tissue by MALDI imaging. Scientific Reports, 6, 22627.
Pubmed: Author and Title
CrossRef: Author and Title
Google Scholar: Author Only Title Only Author and Title

RASBERY, J. M., SHAN, H., LECLAIR, R. J., NORMAN, M., MATSUDA, S. P. T. & BARTEL, B. 2007. Arabidopsis thaliana Squalene Epoxidase 1 Is Essential for Root and Seed Development. Journal of Biological Chemistry, 282, 17002-17013.
Pubmed: Author and Title
CrossRef: Author and Title
Google Scholar: Author Only Title Only Author and Title

ROWAN, M. G. & DEAN, P. D. G. 1972. α-Onocerin and sterol content of twelve species of Ononis. Phytochemistry, 11, 3263-3265.
Pubmed: Author and Title
CrossRef: Author and Title
Google Scholar: Author Only Title Only Author and Title

ROWAN, M. G., DEAN, P. D. G. & GOODWIN, T. W. 1971. The enzymic conversion of squalene, 2(3),22(23)-diepoxide to α-onocerin by a cell-free extract of Ononis spinosa. FEBS Letters, 12, 229-232.
Pubmed: Author and Title
CrossRef: Author and Title
Google Scholar: Author Only Title Only Author and Title

SAINSBURY, F. & LOMONOSSOFF, G. P. 2008. Extremely High-Level and Rapid Transient Protein Production in Plants without the Use of Viral Replication. Plant Physiology, 148, 1212-1218.
Pubmed: Author and Title
CrossRef: Author and Title
Google Scholar: Author Only Title Only Author and Title

SAWAI, S., SHINDO, T., SATO, S., KANEKO, T., TABATA, S., AYABE, S.-I. & AOKI, T. 2006. Functional and structural analysis of genes encoding oxidosqualene cyclases of Lotus japonicus. Plant Science, 170, 247-257.
Pubmed: Author and Title
CrossRef: Author and Title
Google Scholar: Author Only Title Only Author and Title

SCHAEFER, P. C., DE REINACH, F. & OURISSON, G. 1970. The Conversion of Parkeol into its 24,25-Epoxide by Tissue Cultures of Nicotiana tabacum. European Journal of Biochemistry, 14, 284-288.
Pubmed: Author and Title
CrossRef: Author and Title
Google Scholar: Author Only Title Only Author and Title

SCHNEIDER, C. A., RASBAND, W. S. & ELICEIRI, K. W. 2012. NIH Image to ImageJ: 25 years of image analysis. Nat Meth, 9, 671-675.
Pubmed: Author and Title
CrossRef: Author and Title
Google Scholar: Author Only Title Only Author and Title

SPENCER, T. A. 1994. The squalene dioxide pathway of steroid biosynthesis. Accounts of Chemical Research, 27, 83-90.
Pubmed: Author and Title
CrossRef: Author and Title
Google Scholar: Author Only Title Only Author and Title

SUZUKI, H., ACHNINE, L., XU, R., MATSUDA, S. P. T. & DIXON, R. A. 2002. A genomics approach to the early stages of triterpene saponin biosynthesis in Medicago truncatula. The Plant Journal, 32, 1033-1048.
Pubmed: Author and Title
CrossRef: Author and Title
Google Scholar: Author Only Title Only Author and Title

TAMURA, K., STECHER, G., PETERSON, D., FILIPSKI, A. & KUMAR, S. 2013. MEGA6: Molecular Evolutionary Genetics Analysis Version 6.0. Molecular Biology and Evolution, 30, 2725-2729.
Pubmed: Author and Title
CrossRef: Author and Title
Google Scholar: Author Only Title Only Author and Title

THOMA, R., SCHULZ-GASCH, T., D'ARCY, B., BENZ, J., AEBI, J., DEHMLOW, H., HENNIG, M., STIHLE, M. & RUF, A. 2004. Insight into steroid scaffold formation from the structure of human oxidosqualene cyclase. Nature, 432, 118-122.
Pubmed: Author and Title
CrossRef: Author and Title
Google Scholar: Author Only Title Only Author and Title

TIAN, B.-X. & ERIKSSON, L. A. 2012. Catalytic Mechanism and Product Specificity of Oxidosqualene-Lanosterol Cyclase: A QM/MM Study. The Journal of Physical Chemistry B, 116, 13857-13862.
Pubmed: Author and Title
CrossRef: Author and Title
Google Scholar: Author Only Title Only Author and Title

TURINI, F. G., BRÄUCHLER, C. & HEUBL, G. 2010. Phylogenetic relationships and evolution of morphological characters in Ononis L. (Fabaceae). Taxon, 59, 1077-1090.
Pubmed: Author and Title
CrossRef: Author and Title
Google Scholar: Author Only Title Only Author and Title

VAN DER FITS, L., DEAKIN, E. A., HOGE, J. H. C. & MEMELINK, J. 2000. The ternary transformation system: constitutive virG on a compatible plasmid dramatically increases Agrobacterium-mediated plant transformation. Plant Molecular Biology, 43, 495-502.
Pubmed: Author and Title
CrossRef: Author and Title
Google Scholar: Author Only Title Only Author and Title

VAN TAMELEN, E. E. & HEYS, J. R. 1975. Enzymic epoxidation of squalene variants. Journal of the American Chemical Society, 97, 1252-1253.
Pubmed: Author and Title
CrossRef: Author and Title
Google Scholar: Author Only Title Only Author and Title

VAN TAMELEN, E. E., LEOPOLD, E. J., MARSON, S. A. & WAESPE, H. R. 1982. Action of 2,3-oxidosqualene lanosterol cyclase on 15'-nor-18,19-dihydro-2,3-oxidosqualene. Journal of the American Chemical Society, 104, 6479-6480.
Pubmed: Author and Title
CrossRef: Author and Title
Google Scholar: Author Only Title Only Author and Title

WHELAN, J. A., RUSSELL, N. B. & WHELAN, M. A. 2003. A method for the absolute quantification of cDNA using real-time PCR. Journal of Immunological Methods, 278, 261-269.
Pubmed: Author and Title
CrossRef: Author and Title
Google Scholar: Author Only Title Only Author and Title

WIEDERSTEIN, M. & SIPPL, M. J. 2007. ProSA-web: interactive web service for the recognition of errors in three-dimensional structures of proteins. Nucleic Acids Research, 35, W407-W410.
Pubmed: Author and Title
CrossRef: Author and Title
Google Scholar: Author Only Title Only Author and Title

WOJCIECHOWSKI, M. F., LAVIN, M. & SANDERSON, M. J. 2004. A phylogeny of legumes (Leguminosae) based on analysis of the plastid matK gene resolves many well-supported subclades within the family. American Journal of Botany, 91, 1846-1862.
Pubmed: Author and Title
CrossRef: Author and Title
Google Scholar: Author Only Title Only Author and Title

WU, T.-K., WANG, T.-T., CHANG, C.-H., LIU, Y.-T. & SHIE, W.-S. 2008. Importance of Saccharomyces cerevisiae Oxidosqualene-Lanosterol Cyclase Tyrosine 707 Residue for Chair-Boat Bicyclic Ring Formation and Deprotonation Reactions. Organic Letters, 10, 4959-4962.
Pubmed: Author and Title
CrossRef: Author and Title
Google Scholar: Author Only Title Only Author and Title

XU, R., FAZIO, G. C. & MATSUDA, S. P. T. 2004. On the origins of triterpenoid skeletal diversity. Phytochemistry, 65, 261-291.
Pubmed: Author and Title
CrossRef: Author and Title
Google Scholar: Author Only Title Only Author and Title